Present and future changes in winter climate indices relevant for access disruptions in Troms, northern Norway

Anita Verpe Dyrrdal[1], Ketil Isaksen[1], Jens Kr. Steen Jacobsen[2], Irene Brox Nilsen[3]

[1]Department of Research and Development, Norwegian Meteorological Institute, Oslo, 0313, Norway
[2]Institute of Transport Economics, Oslo, 0349, Norway
[3]Norwegian Water Resources and Energy Directorate, Oslo, 0301, Norway

Correspondence to: Anita Verpe Dyrrdal (anitavd@met.no)

Abstract. A number of seaside communities in Troms in northern Norway are vulnerable to sudden weather induced access disruptions due to frequent high impact weather and dependency on one or few roads exposed to avalanches, wind, and challenging road conditions. In this paper we study changes in selected indices describing winter weather known to potentially cause such access disruptions in Troms. A gridded observation-based dataset is used to analyse changes in present climate (1958–2017), while an ensemble of ten EURO-CORDEX climate model simulations are used to assess expected future changes in the same indices, towards the end of the twenty-first century. We focus on climate indices associated with snow avalanches (such as maximum snow amount, snowfall intensity and frequency, and strong snow drift) and slushflows where rainfall during winter is highly relevant. All climate indices are also associated with access disruptions in general, including freeze-thaw cycles described as zero-crossings (temperature crossing 0 °C) that may lead to slippery road conditions. Our results show that there are large climate gradients in Troms and also in detected changes. In our two focus areas, Senjahopen/Mefjordvær in Berg municipality and Jøvik/Olderbakken in Tromsø municipality, we find that the studied snow indices have become more frequent in present climate, while they expect to become less frequent in near and far future, particularly in low elevations where snow cover during winter might become a rarity by 2100. Events of heavy rain during winter are rather infrequent in the present winter climate of Troms, but we show that these events are likely to occur much more often in all regions in the future. Although the likelihood of dry snow-related access disruptions might decrease, wet snow avalanches and slushflows may become more probable in a warmer and wetter climate. However, there are contradicting arguments related to the development of snow avalanches in a changing climate due to the complexity of avalanche release. We find more zero-crossings in most parts of Troms during the last few decades, and this trend is expected to continue for inland regions and high elevations in the future, while coastal and low-lying regions can expect fewer zero-crossings. Strong snow drift, as a combination of snowfall and wind speed, have slightly increased in the two focus areas, but a strong decrease is expected in the future due to less snow. The higher likelihood of water and rainfall-induced hazards and more frequent freeze-thaw conditions calls for careful coordination of climate adaptation, cooperation between different sectors, as well as additional guidance and training of local authorities in regions with highways exposed

to such natural hazards. At the same time, research into the complex relationship between weather and different types of hazards, especially wet snow avalanches and slushflows, is needed.

1 Introduction

5 Since the turn of the century, there has been a considerable increase in the number of rapid mass movements that affect highways in Norway, according to registrations by the Norwegian Public Roads (Statens vegvesen, 2014).
It has been estimated that one fourth of Norway's public roads are vulnerable to snow avalanches and rockfalls (Frauenfelder et al., 2013). Small communities in Troms, northern Norway, are among the most vulnerable to weather induced access disruptions. Both snow avalanches and landslides have led to fatalities in Troms. An analysis of the Norwegian mass

10 movement database http://skredregistrering.no/ (database version December 2019) shows that for the period 1730–2014, 376 casualties were registered in Troms: Snow avalanches resulted in 295 casualties, whereof 121 people were hit in buildings and nine on roads. Since 2014, an additional 12 casualties are registered, according to varsom.no (all were skiing or driving snow mobile). For other landslides, 81 casualties are registered in Troms, whereof 57 in buildings and two on roads.

15 Quite a few highway stretches along alpine mountainsides in Troms are sporadically closed nearly every winter due to climate-induced incidents such as blizzards, heavy snowfalls, strong winds, and avalanches. Several highways in Troms are also being closed in times with imminent avalanche danger, such as polar low pressure alerts. Snow avalanches are among the natural hazards that most frequently lead to highway blockages, in numerous instances for longer periods of time. Also slushflows and ice-fall are among the winter hazards that may lead to dangerous road user situations and sometimes also

20 road outages. Access highways have been regarded as lifelines; connections that health, safety, comfort, and social and economic life depend on (Holand, 2014). Social science studies have revealed that roadside avalanches and winter weather-induced road closures commonly lead to worries about road travel and numerous practical problems for inhabitants, businesses, and the public sector (Hovelsrud et al., 2018; Leiren & Jacobsen, 2018). Although many residents have been able to prepare and adjust to reduce their vulnerabilities to such recurrent lifeline disconnections during the winter (Jacobsen et

25 al., 2016), there might be negative long-term impacts for communities that have been repeatedly isolated and often exposed to risky cold season road travel (Hovelsrud et al., 2018).

The Arctic region, which Troms is part of, has experienced a major change in climate over the past few decades, driven by increasing temperatures (AMAP, 2017; Vikhamar-Schuler et al., 2016; Hanssen-Bauer et al., 2019). For instance, Vikhamar-

30 Schuler et al. (2016) found that five indices describing winter warming events in the Nordic arctic region have increased significantly during the past 50 years. This trend, being stronger in autumn and winter months, is significantly larger than the global average (Cohen et al., 2014), and is expected to continue in the future (e.g. AMAP, 2017). Using a daily interpolated

dataset, Dyrrdal et al. (2012) performed a Norwegian national analysis of past changes in weather variables that can trigger natural hazards. For Troms, they found that the frequency of moderate to strong precipitation events, and the intensity of strong precipitation events, had increased during the period 1957–2010. Snow amounts had increased in colder areas (inland), while in warmer areas (coast and seaside fjord areas) snow amounts were somewhat reduced. Analyzing large snowfalls and the number of snow days revealed similar patterns, but trends were weaker. The number of near-zero events had also increased during the same period.

Whether increasing temperatures and precipitation will lead to lower or higher probability of snow avalanches is much debated, and depends on avalanche type, slope, wind conditions etc. Studies performed using historical data and projections in western Canada did not suggest a substantial increase in avalanches reaching transportation corridors (Jamieson et al. 2017). Results by Sinickas et al. (2016) suggested that natural avalanche occurrence rates over the past 30 years in western Canada had decreased or stayed constant. However, the results were associated with a very high level of uncertainty. On the other hand, Ballesteros-Canovas et al. (2018) states that the transformation of dry snow packs into wet snow packs is decisive for the release of snow avalanches, which explains an increase in wet snow avalanches in Western Himalayas as winters have become milder. Hestnes & Jaedicke (2018) have discussed that global warming altogether will reduce the impact of slushflows and avalanches on humans globally. They explained this reduction with milder weather, shorter winters with less snow and rising snowlines in populated regions. The same study indicated that the total risk due to rapid mass movements will most likely increase.

Castebrunet et al (2014) shred some light on these contradicting arguments, as they projected a general decrease in mean and interannual variability of avalanche activity in the French Alps, with an amplified decrease in spring and at low altitudes. While in winter and at high altitudes they projected an increase because conditions favourable to wet snow avalanches comes earlier in the season. Similarly, Hanssen-Bauer et al. (2019) stated that an increase in heavy snowfall or heavy rain on snow may increase the occurrence of snow avalanches (including wet snow avalanches and slushflows), while a shorter snow season and reduction in the maximum annual snow amounts may decrease the probability of dry snow avalanches. Hanssen-Bauer et al. (2019) and Hanssen-Bauer et al. (2017) still conclude that the probability of wet snow avalanches and slushflows is expected to increase in Norway.

The current study presents past and future changes in selected winter climate indices known to potentially cause access disruptions in Troms, northern Norway. We have focused on the most common access disruptions and selected climate indices which in literature are known to be potential triggers of snow avalanches and slushflows (thus focusing on natural avalanche occurrences), or somehow generate difficult road/transport conditions in exposed coastal and fjord areas in Troms. First, we present the study region and climate (Section 2), we describe the data and method, and identify relevant climate indices (Section 3), before presenting results (Section 4), and wrapping up with discussion and conclusions (Section 5). The

study will supplement social science investigations and advance natural hazard understandings by providing an overview of historical development and projected future changes in climate indices associated with winter season road travel safety and lifeline disruptions in Troms.

2 Study region

5   Troms was until 1st January 2020 the second northernmost county in Norway (see map in Fig.1), located between 68.3° and 70.3° N, but was merged with the neighboring county of Finnmark to form the new *Troms og Finnmark* county. Troms forming a part of the Arctic region, but with a partly sub-Arctic climate. Troms consisted in 2018 of 24 municipalities with a total area of nearly 26 000 km² and around 165 000 inhabitants. The long coast line with thousands of small islands and islets, including some of Norway's large and mountainous islands, meets steep mountains further inland, resulting in a
10   complex topography (see map in Fig.1). Large parts of the population and infrastructure in Troms are located in narrow zones along the seaside, partly in fjords surrounded by steep mountain slopes. The topography, along with geological and meteorological conditions, makes many roads particularly prone to avalanches. Several small but enterprising communities in Troms have recurrently been cut off from the rest of the region. According to Jacobsen et al. (2016), many communities in Troms experience sudden access interruptions nearly every winter due to snow avalanches and slushflows, heavy snowfall,
15   and/or strong winds and drifting snow in these areas. Eckerstorfer et al. (2017) concluded that Tamokdalen in Troms (about 50km south of Focus area 2; see below) has a transitional snow climate (between maritime and continental climates), where also mid-winter rain-on-snow events lead to extensive wet snow avalanche cycles. Eckerstorfer et al. (2017) compared avalanche activity and forecasted avalanche danger during the two winters of 2014-2016, and identified the highest magnitude avalanche cycles when non-persistent weak layers, such as buried new snow and wind-transported snow, were
20   forecasted as avalanche problems.

In the present study we focus particularly on two areas/communities; Focus area 1: Senjahopen/Mefjordvær next to the fjord Mefjorden in Berg municipality, and Focus area 2: Jøvik/Olderbakken next to the fjord Sørfjorden in Tromsø municipality (see Fig.1 for the location of the two focus areas). Both areas lie within or close to an avalanche zone as defined by
25   Norwegian   Water   Resources   and   Energy   Directorate   (NVE;   https://www.nve.no/flaum-og-skred/kartlegging/aktsemdkart/aktsomhetskart-for-snoskred/). In parts of Troms, as much as 50% of roads are located within susceptibility maps for snow avalanches and rockfall (NGI et al., 2013). Numerous road stretches in Troms go along alpine mountain sides and escarpments prone to snow avalanches (Statens vegvesen, 2014), thus also to closures and damages, as well as representing a threat to people's safety. Only along Mefjorden there are 18 known avalanche tracks with
30   runout zones encompassing the access highway for the fishing villages Senjahopen and Mefjordvær (Sjømatklyngen Senja 2017). In our gridded data, Focus area 1 covers 416 grid cells (1x1 km²), ranging from 0 to slightly more than 800 meters

AMSL. Real elevation might be higher due to smoothing in the gridded elevation data. Focus Area 2 is smaller with 162 grid cells, but with steeper topography ranging from 0 to almost 1800 meters AMSL.

The climate in Troms is strongly influenced by the complex topography with large gradients between coast/fjords and inland regions. During the winter season, Troms is characterized by a relatively mild and wet climate in coastal and fjord areas, while the inner parts are cold and dry (see Fig.2). Mean winter temperatures range from slightly above zero along the seaside to around -12 °C in high elevated areas inland. Valley regions in the inner parts of Troms are particularly dry, with mean winter precipitation of less than 200 mm, while values in southern coastal regions reach about 1200 mm. Polar lows, common for this region, can give sudden periods with strong winds and heavy precipitation in winter time.

According to a report on projected climate-related changes, "Troms climate fact sheet" (Hisdal et al., 2017, based on results from Hanssen-Bauer et al., 2017), from the Norwegian Centre for Climate Services (NCCS; klimaservicesenter.no), annual mean temperature in Troms is expected to increase by about 5 °C as approaching the end of the present century (compared to the historical period 1971–2000) under a high emission scenario (RCP8.5), with a slightly larger increase during winter. Annual precipitation is expected to increase by about 15%, with a larger (30%) increase during summer. Further, days with heavy precipitation are expected to become more frequent and with higher precipitation intensity, resulting in an increased probability of precipitation-induced landslides, debris flows, and slushflows The same report states that snow amounts will likely decrease drastically in lower altitudes and episodes of melting will become more frequent in winter, while some higher altitude regions might expect increasing snow amounts towards the middle of the century. From the development of snow amounts alone, we might expect that the probability of both dry and wet snow avalanches in these regions will increase during the first decades, followed by reduction of dry snow avalanches towards the end of the century (Hisdal et al., 2017). How the effects of these changes on local communities and different sectors could play out, is not much studied.

In northern Norway, wind induced hazards represent significant challenges along the coast and some exposed mountain passes. Wind projections are highly uncertain and show no strong indication of change according to Hisdal et al. (2017) and Hanssen-Bauer et al. (2017). However, some studies have shown a change in cyclone density in the region; a study by Bengtsson et al. (2006) indicating that the location and intensity of storms are expected to change considerably in the future while the change in the total number of cyclones will be small. Empirical-statistical downscaling of CMIP5 simulations suggest an increase in storm activity in northern Norway and in the Barents region in the far future (Parding & Benestad, 2016).

3 Data and method

Three weather variables are of main interest in this study, namely precipitation (including snow), air temperature, and wind, and combinations of these. We computed changes in selected indices (see chapter 3.3) based on these weather variables using datasets that cover the recent climate (1958–2017) and projected future climate (2041–2070 and 2071–2100). As most disruptions due to weather occur during the extended winter season, this is our season of focus. Winter season is defined here as the months October through April (212 days in total).

3.1 Gridded observation-based data

To obtain spatially continuous information on the recent climate, the Norwegian Meteorological institute (MET Norway) provides gridded datasets of daily mean, minimum and maximum temperature (T, Tmin, Tmax) and daily precipitation sum (P) for the Norwegian mainland. The dataset, referred to as "seNorge", is based on observations interpolated to a 1x1 km grid covering the period 1957–present. Different versions of seNorge exist, based on different interpolation methods and input data. For temperature, we here analysed seNorge1 (e.g. Tveito et al., 2002) as it includes minimum (Tmin) and maximum temperature (Tmax) from which we calculated zero-crossings. seNorge1 temperature was developed through residual kriging using terrain and geographic position to describe the deterministic component. For precipitation, however, we use seNorge2 (Lussana et al. 2018), based on Bayesian spatial interpolation and Optimal Interpolation (OI) to propagate information from coarser to finer scales. Snow variables, including daily total snow water equivalent (SWE) and fresh snow water equivalent (FSW; change in SWE from one day to the next), was computed from seNorge1 T and P using the seNorge snow model v1.1.1 (Saloranta, 2014). This uses a precipitation/degree-day snow model with a snow routine similar to the HBV model (Bergström 1992), which is described in Engeset et al. (2004). In seNorge snow model v1.1.1 a temperature-independent melt term is added to the temperature-dependent degree-day term, while the melt threshold temperature is kept at 0 °C. The new melt term is proportional to the potential solar radiation, thus varying with the combination of latitude and time of the year. Saloranta (2014) found that the average station-wise median bias for snow depth from the seNorge snow model v1.1.1 lies between –12 to +17 % all the way from January to the end of April. Since precipitation from seNorge2 is used as input in the snow model, the gridded snow products are referred to as seNorge v2.0.1. Hereby, we refer to all seNorge-datasets as seNorge, followed by the variable of interest, for instance: seNorge Tmax. seNorge is an operational product updated every day, and available on www.senorge.no, and provides important input to the avalanche forecasting in Norway presented on www.varsom.no.

For wind, a dataset of daily mean 10-meter wind speed (FF), named KliNoGrid, is available on a similar grid as seNorge for the period 1957–2015. This dataset is downscaled from a high-resolution (10 km) hindcast of wind and waves for the North Sea, the Norwegian Sea, and the Barents Sea (NORA10; Reistad et al., 2011), evaluating relatively well along the coast of

Norway. The downscaling was performed with a quantile mapping approach (Bremnes, 2004) to match the climatology of the high-resolution numerical weather prediction model (AROME-MEtCoOp, Müller et al., 2017). KliNoGrid is available for public download at https://thredds.met.no/thredds/catalog/metusers/klinogrid/KliNoGrid_16.12/FFMRR-Nor/catalog.html.

3.2 Future projections

To assess expected future climate development, we used projections from climate models. The model chain starts with low-resolution General Circulation Models (GCMs) covering the entire earth, which output is used into Regional Climate Models (RCMs) that simulates climate on a finer grid over a region. Finally, an ensemble of ten simulations from the EURO-

10 CORDEX project (Jacob et al., 2014), representing different combination of GCMs and RCMs, has been downscaled to a similar grid as the seNorge-grid described above (1 km horizontal resolution). Due to the systematic biases in the climate model output and their mismatch in scale with impact models data requirement, a post-processing is necessary to obtain plausible time series for use in local impact studies. The downscaled EURO-CORDEX ensemble for the entire period 1971–2100 was bias-adjusted towards seNorge version 1.1 for daily mean temperature and daily precipitation sum (Wong et al.,

15 2016), while for daily mean wind speed the KliNoGrid dataset described above was used as reference for the bias-adjustment. An empirical quantile mapping method was used in the bias-adjustment of precipitation and wind. For mean temperature the same method was used on the anomalies, while for minimum and maximum temperature a quantile delta mapping method (Cannon et al., 2015) was used on the projections.

20 We refer to the corrected datasets of temperature, precipitation and wind as "EUR11-Nor1", where EUR11 stands for EURO-CORDEX with 0.11° resolution, Nor stands for Norway and 1 stands for 1 km resolution. Temperature and precipitation were then used to force a spatially distributed, gridded hydrological model (the HBV model) (Wong et al., 2016) to generate daily time series of different hydrological components. Here we focused on daily SWE, from which we also computed daily FSW. The Norwegian government recommends, as a precautionary principle, using the high emission

25 scenario when assessing the effects of climate change (Norwegian Ministry of Climate and Environment, 2013), thus we only analysed projections from the RCP8.5 emission scenario. Datasets of precipitation, temperature and hydrological variables described here contribute to the natural scientific basis for climate adaptation in Norway, as described in Hanssen-Bauer et al., 2017). Some of them (precipitation, daily mean, maximum and minimum temperature and SWE), are available through the Norwegian Climate Data Store: https://nedlasting.nve.no/klimadata/kss. The ten GCM-RCM combinations in

30 the EURO-CORDEX ensemble are shown in Table A1 in the Appendix. In the results, we report on the ensemble mean of the ten simulations, not individual model simulations.

3.3 Climate indices

We identified indices describing weather elements which in literature are known to be potential triggers of snow avalanches and slushflows, or somehow generate difficult conditions for road users. For frequency indices, we pragmatically selected the thresholds to facilitate a trend analysis, but we believe that the pattern of changes for low-threshold events can be transformed to higher-threshold events. The final choice of selected indices was also influenced by the availability of the parameters as gridded data, for both historical and future periods. Of rapid mass movements the indices analyzed here are mostly relevant for snow avalanches and slushflows. For weather induced access disruptions in general we chose indices that often lead to difficult road and driving conditions. The derived indices were identified from literature referred to in the following text, and presented in Table 1 below.

In this paper, we use snow avalanches as a common term for all kinds of snow avalanches (including slushflows), and landslides as a common term for rock avalanches (including rockfall) and debris avalanches (debris flows, mudflows), unless where a specification into type is needed. We have followed the classification from Kristensen et al. (2015).

Jaedicke et al. (2008, 2009) coupled 20 000 historical landslide and avalanche events in Norway. Combining avalanche and meteorological data for the period 1961 to 2005 to 41 meteorological elements. These data sets were then used in a classification tree analysis to identify the most relevant meteorological elements causing avalanches and landslides. Results showed that snow avalanches had the highest correlation with meteorological elements such as wind and precipitation, while rockfall showed the lowest correlation (Jaedicke et al. 2008). The study also revealed that the most important elements triggering landslides or avalanches varied spatially over Norway. While 1-day precipitation was the most important trigger for snow avalanches in the coastal south-western part of the country, both wind and precipitation played an important role in northern Norway. Sandersen et al. (1996) found that particularly strong storms with heavy rain and snowfall frequently initiate landslides and snow avalanches, and concluded that debris and slushflows in Norway are often initiated at times of high water supply from intense rainfall and/or rapid snowmelt. NVE (2014) indicated a critical threshold of 40 mm/day of total rain+melt, given by field experience and measurements. Here we studied winter rainfall events (precipitation amount on days with $T > 0°C$) exceeding a threshold of 10 mm/day. During such rainfall events one can expect an extra contribution to water supply through melting. In addition to potentially leading to slippery road conditions due to low surface temperatures and/or freezing at night, such winter rain events can lead to the formation of thick internal ice layers in the existing snowpack, which again inhibits for instance reindeer from foraging and limits vegetation growth (e.g. Vikhamar-Schuler et al., 2016; Pall et al., 2019).

NVE (2014) has stated that at least 0.5 m of fresh snow in 2–3 days, along with strong winds, is required to trigger a snow avalanche of significant size. This is in agreement with Schweizer et al. (2003) who stated that about 30–50 cm of

accumulation of a new snow is critical for naturally released avalanches. The combination of wind speed and fresh snow can be defined as a so-called snow drift factor, which have proven high skill in avalanche prediction. Davis et al. (1999), Hendrikx et al. (2005) and Kronholm et al. (2006b) all used classification trees to show that snow drift factors rate among the top indices for avalanche activity. Davis et al. (1999) used the expressions from Pomeroy and Gray (1995) to derive the wind drift factor as the product of the 24-hour snowfall and wind speed to the fourth power (see Equation 1 below):

$$snow\ drift\ \left[mm\left(\frac{m}{s}\right)^4\right] = precipitation\ [mm] * (wind\ speed)^4\ \left[\frac{m}{s}\right] \qquad (1)$$

Here we adopted this definition of snow drift, using 1-day snowfall (FSW-1d) and daily mean wind speed (FF).

Due to the large uncertainties associated with wind, and particularly the high influence from local conditions, we selected the grid cells of highest wind exposure in each focus area (6/8 grid cells in Focus area 1/2, respectively). We computed the snow drift factor according to Equation 1 above, calculated the number of events where the snow drift factor exceeds the 90th percentile (p90), and averaged over all selected grid cells within the focus area before computing the percentage change.

It is accepted that the most high-risk temperature when it comes to slippery roads is when the road surface is around or just below 0 °C (Andersson and Chapman 2011; Gustafson, 1983; Thornes, 1991). Here, a zero-crossing is defined as Tmin < 0 and Tmax > 0 on the same day (Geiger et al., 2012; Kerguillec, 2015), meaning a fluctuation between freezing and thawing conditions. A better index for slippery road conditions could have included surface temperature and humidity (Gustafson, 1983), but these variables were not available as gridded fields. Besides, surface temperatures on roads depend on the thermal conductivity of the road pavement, which is not known. In lieu of surface temperatures, we decided to use maximum and minimum temperatures taken at 2 m height as a proxy.

Table 1: Description of selected climate indices.

Climate index	Dataset Present climate	Dataset Future climate	Details / Abbreviation	Associated hazard
Maximum snow amount	seNorge SWE	EUR11-Nor1-SWE	WM-SWE	Snow avalanche
Maximum snowfall intensity 1 and 5 days	seNorge FSW	EUR11-Nor1-SWE	WM-FSW-1d WM-FSW-5d	Snow avalanche, slippery roads and difficult driving conditions
Frequency of heavy snowfall	seNorge FSW	EUR11-Nor1-SWE	FSW-1d > 5 mm	Snow avalanche, slippery roads and difficult driving conditions
Frequency of zero-crossings	seNorge Tmin/Tmax	EUR11-Nor1-T	Tmax > 0 and Tmin < 0 on the same day, abbr: zero-crossings	Slippery roads and difficult driving conditions
Frequency of winter rain events	seNorge T seNorge P	EUR11-Nor1-T EUR11-Nor1-P	Winter rain > 10 mm	Slushflows, snow avalanches, slippery roads and difficult driving conditions
Frequency of strong snow drift	KliNoGrid FF seNorge FSW	EUR11-Nor1-FF EUR11-Nor1-SWE	Snow drift > p90	Snow avalanche and difficult driving conditions

3.4 Method

Past trends in winter maxima and peak-over-threshold events were assessed through the rank-based nonparametric Mann-Kendall trend test (R-package Kendall) to identify positive and negative trends, and evaluate their statistical significance at a 5% level. Mann-Kendall tests the null hypothesis that the data are independent and identically distributed, and is well suited to study hydrometeorological time series, as these are usually non-normally distributed (Yue & Pilon 2004). In addition, we computed the percentage change between the mean values from the first 30-year period (1958–1987) and the last 30-year

period (1988–2017). For snow drift which is only computed for selected grid cells in the two focus areas, no trend analysis is performed.

To assess expected future change, we computed the percentage change in temporal mean between the historical period 1981–2010 and two future periods; 2041–2070 (near future) and 2071–2100 (far future) through the methods described above. For both past and future changes, we extracted mean spatial statistics over the whole of Troms and for the two focus areass and present these in a separate table. Within each focus area we additionally identified two elevation bands representing likely snow avalanche release zones (> 700 meters AMSL in focus area 1 and between 1000 and 1300 meters AMSL in study area 2) and likely avalanche run-out zones (< 200 meters AMSL), and report on changes computed for grid cells falling into these elevation bands. All roads in the study areas are located below 200 meters while the high elevation band is defined a collaboration with local avalanche experts.

In the attempt to identify the period for which snow avalanches may become a larger threat, and at which point they become a decreasing threat, we investigated the past and projected development in maximum snow amounts for different elevations. We also analysed future changes in the median elevation where winter maximum SWE is lower than certain thresholds; 100 mm, 200 mm and 400 mm. Due to the large gradients in climate variables in Troms, the latter analysis is performed for separate inland and coastal/seaside regions as defined in Fig.1.

4 Results

In Fig.3 we show how winter temperature and precipitation has varied over the last 150 years at a meteorological station in Tromsø, the administrative center of the municipality. Winter temperature fluctuates between –5 and 0.5 °C, and winter precipitation typically fluctuates between 250 and 950 mm. The temperature time series indicate multi-decadal variability, with a relatively cold period between the 1910s and the 1920s, a relatively warm period during the subsequent two decades, a temperature decrease from the 1950s to the 1960s, and thereafter a general temperature increase. Other parts of the Arctic have a similar pattern (e.g. Polyakov et al. 2003, AMAP 2017). The linear trend during the 60-year period 1958–2017, which is the period we focus on in the current study, shows a significant increase in winter temperature (0.26 °C/decade) and a moderate increase in winter precipitation (2.2 %/decade) in Tromsø.

Further, we present results for each climate index separately, starting with historical and future changes the whole of Troms. We proceed with results from the who focus areas as presented in Table 2, including changes in elevations relevant for avalanche release zones (high elevations) and run-our zones (low elevations), for the historical period and the two future period. In Table 2 we also report on the mean values for the period 1981–2010 for reference.

4.1 Changes in maximum snow amount

Fig.4 shows mean winter maximum snow water equivalent (WM-SWE) and the spatial trends and changes during the study period 1958–2017. The largest values of WM-SWE are found in higher elevations (see map in Fig.1) near the coast and along the fjords, while decreasing towards the Swedish border to the east (Fig.4a). In Fig.4b, significant positive trends are seen inland and in the north-eastern part of Troms, with an increase of 20–60% from the first to the last 30-year period (Fig.4c). Some coastal regions, especially in the southern and north-western outermost areas, are dominated by significant negative trends in WM-SWE. These areas show a decrease of 20–40% between the first 30-year period (1958–1987) and the last 30-year period (1988–2017).

Fig.5 presents projected percentage changes in WM-SWE for near (2041–2070) and far (2071–2100) future, as given by EUR11-Nor1-SWE. Changes are mainly negative, with strong gradients from coast (largest decrease) to inland (weakest decrease). As expected, the changes become larger with time. The largest projected decrease, in the islands along the coast, are in the order of 60–80% for near future (Fig.5a) and 80–100% for far future (Fig.5b).

Fig.6 shows the same change in WM-SWE for past and future climate, but for different elevation levels. Again, we see that changes in WM-SWE are mainly positive in the past, but become negative in the future. The higher elevated areas show the largest increase in the past, and the smallest decrease in the future, explained by the lower temperature in these regions. At some point between present and near future, the temperature in these region will, however, reach levels that give declining snow amounts also here. This is further investigated in Fig.7, showing the median elevation where maximum snow amounts stay below certain thresholds (100, 200 and 400 mm). Due to the strong gradients in Troms, we analyze projected changes in WM-SWE for coastal regions (Fig.7a) and inland regions (Fig.7b) separately (see map in Fig.1), thus elevation on the x-axis differs. Median elevation in both regions increase as approaching the end of the century, more so in the coastal region and particularly for WM-SWE < 100 mm, meaning that we need to go to higher and higher altitudes to find snow in the future. Since the elevations are strictly increasing as of 2040, it is likely that the turning point from increasing to decreasing snow amounts occur prior to 2040, at least in terms of WM-SWE. This is supported by the 1981-2010 mean values (indicated as triangles in Fig.7) being lower than values in 2040, except in lower elevations inland where 1981-2010 values are higher. As shown in Fig.4, WM-SWE has increased in the inland region during 1957-2017, and this trend has likely continued longer and/or been stronger in lower elevations. The narrowing range between smaller and larger snow amounts indicates a stronger elevation gradient for WM-SWE as winter precipitation increases, particularly in low elevations and coastal regions where winters are comparatively mild. . This might be explained by the fraction of rain and degree of snow melt in lower versus higher elevations differing more in the future, giving a stronger decrease in the low to medium elevations.

In focus area 1 we compute a 17% increase in WM-SWE (Table 2), with significantly higher values (30%) in the high elevation band, and lower values (4%) in the low elevation band. This is similar for study area 2, but with a mean increase of only 10%. In the future, Focus area 1 is expected to have much less snow-related challenges, with nearly 70 (90)% decrease in the maximum snow amount in near (far) future. This will reduce maximum snow amounts from about 363 mm in the current climate (1981–2010) to only 36 mm by the end of the century. Focus area 2 shows a decrease of 47 (70)% in near (far) future. While decreases are similar for high and low elevations in Focus area 1, a decrease of 85% is expected in low elevations of Focus area 2 towards the end of the century, versus only –57% in high elevations.

4.2 Changes in maximum snowfall

The mean, trends and changes in winter maximum fresh snow water equivalent (WM-FSW), are shown in Fig.8 for 1-day duration (WM-FSW-1d) and in Fig.9 for 5-day duration (WM-FSW-5d), where FSW is the change in SWE from one day to the next. There are no large areas of significant negative trends in these variables, but decreases of about 10% in WM-FSW-1d are evident inland and in some coastal areas in the south and the north-west (Fig.8c). These areas of weak negative trends become smaller with the longer duration; for WM-FSW-5d only islands north of the city Tromsø inhibit weak negative trends (Fig.9b). Positive trends, some of them significant, dominate the middle regions and the coastal areas north-east and far south. Areas of positive trends increase with the longer duration. Increases of 20–40% (Fig.8c) and 30–50% (Fig.9c) are seen for WM-FSW-1d and WM-FSW-5d, respectively, except a small area of even stronger increase in the far north-east.

WM-FSW-1d and WM-FSW-5d in the future (Figures 10–11) are projected to decrease with a similar spatial pattern as WM-SWE, i.e. most along the coast and more in far future compared to near future. Projected decreases along the coast in far future range between 30 and 60% for WM-FSW-5d and between 40 and 70% for WM-FSW-5d.

The largest change in the past is seen for WM-FSW-5d with an increase of 31%, and similar numbers for both low and high elevation bands. Focus area 2 only had an increase of 15%, but with 24% increase in high elevations and only 5% in low elevations. By the end of the century Focus area 1 can expect a decrease of 57% and 68% for WM-FSW-1d and WM-FSW-5d, respectively, while Study area 2 can expect a smaller decrease of 30% and 36%

4.3 Changes in heavy snowfall events

The frequency of heavy snowfall events (FSW-1d > 5 mm) is presented in Fig.12, showing a similar spatial distribution of trends as WM-SWE but with smaller areas of significant trends. Mean values for the extended winter season (Fig.12a) range from about 10 events (far inland) to about 50 events (at some high-elevated areas near the coast). Significant negative trends

are found in and around Ringvassøya (Fig.12b), an island encompassing Tromsø municipality, with decreases of around 20% from the first 30-year period to the last (Fig.12c). Southern areas inland and coastal areas in the north-east show significant positive trends, with 30–50% more events in the last period compared to the first.

5   The frequency of heavy snowfall events is expected to decrease in the whole region in the future (Fig.13), similar to other snow indices, by up to 60–70% in near future and up to 100% in far future along the coast. This means that in these regions most heavy precipitation events will come as rain instead of snow as approaching the end of the century, as a consequence of milder winters.

10   From Table 2 we find that a 17% and a 4% increase in FSW-1d > 5mm has occurred in 1958–2017 in Focus area 1 and 2, respectively. However, in both near and far future these events are expected to decrease by up to 89% in Focus area 1 towards the end of the century. Comparing to mean values for the reference period 1981–2100, this means a decrease from 38 to about 4 events on average. A smaller decrease of 64% towards the end of the century is expected in Focus area 2.

15   **4.4 Changes in zero-crossings**

Fig.14 shows a clear increase in the number of zero-crossings in the entire Troms during 1958–2017, with large parts being dominated by significant positive trends (Fig.14b), reflecting increasing temperatures over the period. The frequency of events for the extended winter season (212 days in total) increases westwards, with 10–50 events inland to 70–90 events along the coast and in valley bottoms (Fig.14a). The percentage increase between the first and the last 30-year period ranges
20   from about 10% to 40%, with no obvious spatial pattern (Fig.14c), apart for a smaller change in valley bottoms.

Similar to the frequency of zero-crossings in the present climate, projected changes in zero-crossings (Fig.15) also show an increase in many areas, reflecting that temperatures will rise to the zero degree threshold for a longer period. However, in the mildest areas along the coast, where mean winter temperatures are already close to zero in the present climate, these crossing
25   events will become less frequent. Both increases and decreases are expected to become stronger towards the end of the century.

In Focus area 2 zero-crossings have become more frequent, with an increase of 24%, as opposed to only 5% in Focus area 1 (1981–2010). However, high elevations of Focus area 1 have experienced an increase of 18%. These events are expected to
30   decrease in Focus area 1 in far future (–18%), while an increase of 52% is expected in Focus area 2. Numbers for high and low elevations differ significantly in this area, with almost a doubling of events in higher elevations and a slight decrease in low elevation in the far future. A decrease of 39% is expected in the lower elevations of Focus area 1, meaning that slippery road conditions will become less frequent in these areas during winter.

4.5 Changes in winter rain events

Fig.16 shows changes between the first and the last 30-year period of 1958–2017 for mean number of days per winter with rainfall exceeding 10 mm. Mean values of winter rain > 10 mm range between 0 (far inland) to about 30 events on the southeast coast (Fig.16a). There has been an increase of such events in the whole of Troms, with significant positive trends in many coastal regions (Fig.16b).

Winter rain events have been rare in Troms in the past, but Fig.17 shows that the frequency of winter rain > 10 mm is projected to increase everywhere in Troms. Increases of up to 400% are expected in some inland regions (Fig.17b), while in coastal regions show increases of up to 100% towards the end of the century.

Focus area 1 (2) experience about 70% (42%) more heavy winter rain events today compared to the first 30-year period (Table 2). Approaching the end of the century the largest change is expected in Focus area 2, with a 361% increase in high elevations. However, in these areas there were only 1–2 events with rain > 10 mm/day in the period 1981–2010, meaning that an increase of 361% would result in 6–7 events by the end of the century.

4.6 Changes in snow drift

For changes in the snow drift factor we only have numbers for the two focus areas as means over selected grid cells particularly exposed to wind. Events of snow drift > p90 have increase by 16% and 10% in Focus area 1 and 2, respectively. Focus area 2 can expect slightly larger changes in the future, with a decrease of 89% towards the end of the century. With a mean number of strong snow drift events of 21 in the current climate, an average of about two events each year is expected in 2071–2100.

Table 2: Estimated changes in climate indices between two 30-year periods in the two focus areas, based on spatial mean values. In parenthesis we present the change in the lower and higher elevation bands, respectively. Values for snow drift are only based on selected grid cells in high and wind exposed elevations. All values are in %. Past change refer to the change between the first and the last 30-year period during 1958–2017 (for wind: 1958–2015). Change in near (far) future refers to change between 1981–2010 and 2041–2070 (2071–2100).

Climate index	Past changes Whole region (low, high) Reference value (1981–2010)		Changes in near future Whole region (low, high)		Changes in far future Whole region (low, high)	
	Focus area 1	Focus area 2	Focus area 1	Focus area 2	Focus area 1	Focus area 2
WM-SWE	**17** (4,30) 363 mm	**10** (0,12) 426 mm	**-69** (-71, -60)	**-47** (-63, -32)	**-89** (-91, -85)	**-70** (-85, -57)
WM-FSW-1d	**26** (28, 27) 24 mm	**12** (9, 16) 27 mm	**-30** (-34, -21)	**-16** (-31, -4)	**-57** (-66, -38)	**-30** (-55, -11)
WM-FSW-5d	**31** (32, 34) 56 mm	**15** (5, 24) 61 mm	**-37** (-44, -23)	**-19** (-35, -7)	**-68** (-77, -48)	**-36** (-64, -16)
FSW-1d > 5 mm	**17** (15, 22) 38 events	**4** (-1, 7) 37 events	**-65** (-73, -48)	**-39** (-60, -24)	**-89** (-94, -76)	**-64** (-85, -48)
Zero-crossings	**5** (0, 18) 79 events	**24** (20, 28) 67 events	**7** (-13, 38)	**43** (9, 60)	**-18** (-39, 23)	**52** (-4, 90)
Winter rain > 10 mm	**70** (75, 36) 13 events	**42** (37, 36) 5 events	**43** (30, 68)	**88** (42, 123)	**62** (39, 125)	**207** (69, 361)
Snow drift > p90	**16** 22 events	**10** 21 events	**-61**	**-67**	**-85**	**-89**

5 Discussion and conclusions

Our analyses of past development point to areas in Troms where snow amounts and heavy snowfall events have increased, thus increasing the potential for dry snow avalanches. These areas are characterized by relatively low temperatures, typically at high altitudes and in some inland regions, and our results correspond well with those of Dyrrdal et al. (2012). Ensemble mean projections of snow conditions in the future period 2040–2100, however, show a decrease in maximum snow amounts and heavy snowfall intensity and frequency in all of Troms, particularly in low altitude regions, indicating that the transition from increasing to decreasing dry snow avalanche likelihood takes place before 2040 even in the highest and coldest areas. This is in line with observed changes in the European Alps (Naaim et al. 2016), as well as for predicted changes in the

Nordic Arctic region (Hanssen-Bauer et al. 2019). However, as pointed out by Hestnes and Jaedicke (2018), a general reduction of slushflows and avalanches might be realistic in a warmer climate with a shorter winter season and less snow.

Events of winter rain > 10 mm occur relatively seldom in the present climate, still, they have already become more frequent in Troms in the last decades. This is in line with findings by Pall et al. (2019), who showed that rain-on-snow events were more frequent during winter months in 1981–2010 compared to 1961–1990. Over the next few decades, our results indicate that heavy winter rain events are likely to increase in all regions, although high percentage increases are partly explained by low relative numbers, thus absolute changes are restrained to 8–10 more events by the end of 2100. A likely explanation of more frequent winter rain events is obviously milder winters, but the amount of water vapor available is also likely to be higher in a warmer atmosphere. Another plausible contributor to more water supply is the lengthening of the snow melt season into the winter season defined in current climate. In the period 1971–2000, mean number of snow days were between 180 and 270 in Troms, thus covering the whole winter season (Oct–Apr) of 212 days. A decrease of 60–180 days by 2071–2100 under emission scenario RCP8.5 is expected, depending on elevation (Hanssen-Bauer et al., 2017). Consequently, very few or no areas will have a full snow season and the snow melt season will start earlier and contribute more to water supply during winter, as long as snow is available. More rain during winter and more snow melt may point to increased likelihood of wet snow avalanches and slushflows in the areas of Troms. However, Hisdal et al. (2017) states that slushflows will occur earlier in the spring and become less frequent towards the end of this century due to less snow available. In addition, other studies show that an increase in the liquid water content of snow in motion will tend to reduce friction, increasing avalanche runout distances (Naaim et al. 2013), while conserving high-impact pressures even close to the point of rest (Sovilla et al. 2010) and, thus, high damage potential (Ballesteros-Cánovas et al., 2018). The contradicting arguments pointed out here underline the complexity of avalanche release and the large uncertainties associated with the future development of such hazards under climate change. In this regard, we would like to urge further studies on expected future avalanche activity covering different avalanche types.

Changes in zero-crossings indicate shifts in slippery road conditions. Although our definition a zero-crossing refers to the fluctuation of air temperature across zero, and additional information about the surface temperature would have given a better representation of slippery conditions, the change pattern shown here would likely be close to a change pattern of surface temperatures. For the low-lying seaside regions of Troms, with several access roads, we primarily expect changes in zero-crossings in the beginning of winter (Oct–Nov) and the end of winter (Apr–May). These seaside regions have mean temperatures close to 0 °C in the shoulder months in the present climate, and even a small temperature increase will therefore lead to large changes in zero-crossings. Fewer zero-crossings are expected both prior to and after the winter season, with the strongest change expected in October and May. In these shoulder months, the change signal of fewer crossings is expected to reach far inland, while for other months, it is limited to the coast. Increases in zero-crossings are limited to regions far inland, at altitudes above approximately 600–700 AMSL from November to April. Dyrrdal et al. (2012) also

found positive trends in near-zero events in the entire region (1957–2010), but trends were mainly statistically non-significant, except in small regions along the border between Norway and Sweden. Their analysis was based on daily mean temperature and ended in 2010. Thus the results here are more robust and the pronounced positive trends in the entire Troms seem realistic. Trends are, however, sensitive to the choice of period. This is shown by Kerguillec (2015), who studied zero-crossings in Norway using daily thermal data from 20 meteorological stations for the period 1950–2013, including two stations in Troms. For these two stations, the frequency of zero-crossings increased during the periods 1970–1979 and 1990–1999 but decreased in the 1980s. Kerguillec (2015) claims that a strong negative NAO (North Atlantic Oscillation) index generally increases zero-crossings in seaside regions, particularly those in Troms. According to Gillett et al. (2013), most climate models simulate some increase in the winter NAO index in response to increasing concentrations of greenhouse gasses. If this is true, we might speculate that more frequent positive NAO in the future might give fewer zero-crossings in Troms. This is indeed what we find for seaside areas, while inland areas and mountains are expected to have more zero-crossings in the future compared to present climate. These are the coldest areas in the present, and an increase in temperature will bring winter temperatures closer to zero.

Our two focus areas, Senjahopen/Mefjordvær (Mefjorden) and Jøvik/Olderbakken, have and will experience many of the same changes in climate indices relevant for access disruptions. However, as Focus area 1 is more exposed towards the ocean and any incoming weather, we find that changes in snow amount and frequency of snowfall events are larger here compared to Focus area 2. In both areas an increase in all studied snow-related variables has occurred in the last decades, more so in higher elevations, while a decrease is expected towards the end of this century and particularly in low elevations. This means a potential for less dry snow-related access disruptions in the future, while wet snow avalanches and slushflows may increase. In the far future, we have shown that zero-crossings and events of winter rain > 10 mm are projected to increase, and more so in Focus area 2. In areas where there is still a significant amount of snow in 2071–2100, weather described by the studied indices might become a larger threat as potential triggers of avalanches and challenging road conditions. Our findings support to a large degree the Troms climate fact sheet of Hisdal et al. (2017), which states that slushflows will become an increased threat in Troms in the future, and that snow avalanches may become a larger threat in the short run due to more rain-on-snow events, while reduced snow amounts in the long run will decrease the risk for snow avalanches.

We have shown that strong snow drift, computed from snowfall and wind speed, have slightly increased in the two focus areas, but that a strong decrease is expected in the future. There is no evidence for large changes in wind activity in our regions and wind projections are associated with a high degree of uncertainty, of which a large part is related to their positioning of storm tracks (e.g. Zappa et al., 2013). Storm track activity in the Northern Hemisphere is well correlated with NAO and the North Pacific Oscillation (PNA) (e.g. Lee et al., 2012). Positive anomalies of the NAO Index are associated with a strengthening of the mid-latitude westerly flow over the North Atlantic, which manifests itself as an intensification

and poleward deflection of the North Atlantic mid-latitudinal storm track (e.g. Sorteberg et al., 2013). Thus, an increase in the winter NAO index, as suggested by Gillett et al. (2013), might result in more frequent storms at our latitudes. However, an obvious reason for fewer strong snow drift events is the lack of snow when approaching 2100, as discussed above.

5   Although observation based datasets are associated with uncertainty, especially due to relatively sparse measurements in a complex terrain, future projections have a number of uncertainty aspects. As table A1 reveals, the ensemble is somewhat biased towards a few GCMs (particularly EC-EARTH) and RCMs (particularly RCA), representing a weakness along with the relatively limited number of simulations. Other sources of uncertainty associated with future climate projections of temperature and precipitation include emission scenario, natural climate variability, shortcomings in our understanding of the

10   climate system, which results in climate models reproducing certain processes incorrectly, and limited capacity of supercomputers (Hanssen-Bauer et al., 2017). Kotlarski et al. (2014) report that for instance the RCA model seems to have a cool and wet bias over the Scandinavian region during the winter (DJF) season, meaning that future projections in the current study could be biased towards larger snow amounts. Projections for Norway are bias-adjustment (see Section 3.1), thus systematic biases are removed. Still, only one method of bias-adjustment is used. Further, uncertainties in the hydrological

15   modelling, mostly related to parameterization and the fact that only one hydrological model is used, affects snow parameters.

In a changing climate it is particularly important to identify areas of increased vulnerability and risk of weather-induced hazards. As we, in the current study, have focused on only a few selected climate indices, future studies might include other relevant indices. We note that reported avalanche activity has become more detailed during the last years, and new avalanche

20   monitoring stations are in operation closer to typical run-out zones. This will provide new insight into triggering weather conditions, which can be used to study the links between weather and avalanche release.

Seaside communities with access highways exposed to natural hazards, such as Focus area 1 and Focus area 2, require specific measures for climate adaptation that sustains the safety of local citizens and businesses. According to Kalsnes et al.

25   (2016) there is a lack of technical competence and capacity in several municipalities that, by Norwegian law, are responsible for preventive measures and risk management associated with weather-induced hazards. Literature on weather vulnerabilities and climate adaptation recommends increased public sector coordination (Leiren & Jacobsen, 2018), but the different mandates of responsible public authorities sometimes clash. With a higher likelihood of water and rainfall-induced hazards and more frequent freeze-thaw conditions in certain inland areas, a better coordinated climate adaptation, cooperation

30   between different sectors, as well as guidance and training of local authorities will be crucial.

Data availability: Gridded observation-based data, described in Section 3.1, is available upon request to the Norwegian Meteorological institute or the corresponding author. Future projections downscaled to a 1x1 km grid over Norway, as described in Section 3.2, are available for download on https://nedlasting.nve.no/klimadata/kss (in Norwegian).

Author contribution: AVD designed the experiments in close collaboration with KI, and carried out most of the analyses. IBN provided data and code for analysing zero-crossings. JKSJ supervised the process and provided the social scientific perspectives. AVD prepared the manuscript with contributions from all authors.

Competing interests: The authors declare that they have no conflict of interest.

Acknowledgements: This study was funded by the Research Council of Norway through the Climate Research Programme KLIMAFORSK (ACHILLES, project no. 235574).

10   ACHILLES is a part of CIENS (Oslo Centre for Interdisciplinary Environmental and Social Research), a strategic research collaboration of seven independent research institutes and the University of Oslo.
We thank Graziella Devoli for analysing casualties in the mass movement database.

References

15   Andersson, A. and Chapman, L.: The use of a temporal analogue to predict future traffic accidents and winter road conditions in Sweden. Met. Apps, 18: 125–136. doi:10.1002/met.186, 2011

AMAP: Snow, Water, Ice and Permafrost in the Arctic (SWIPA) (2017). Arctic Monitoring and Assessment Programme (AMAP), Oslo, Norway. xiv + 269 pp, 2017

Ballesteros-Cánovas, J.A., Trappmann, D., Madrigal-González, J., Eckert, N., and Stoffel, M.: Climate warming enhances snow avalanche risk in the Western Himalayas. Proceedings of the National Academy of Sciences Mar 2018, 115 (13) 3410–3415; DOI: 10.1073/pnas.1716913115, 2018

25   Bengtsson, L., Hodges, K.I. and Roeckner, E.: Storm tracks and climate change, Journal of Climate, 19, 3518–3543, 2006

Bremnes, J. B.: Probabilistic wind power forecasts using local quantile regression. Wind Energ., 7: 47–54. doi:10.1002/we.107, 2004

Cohen, J., Screen, J., Furtado, J. *et al.* Recent Arctic amplification and extreme mid-latitude weather. Nature Geosci, 7, 627–
30   637, doi:10.1038/ngeo2234, 2014

Cannon, A.J., Sobie, S.R., and Murdock, T.Q.: Bias Correction of GCM Precipitation by Quantile Mapping: How Well Do Methods Preserve Changes in Quantiles and Extremes? Journal of Climate, 28, 6938–6959, doi:10.1175/JCLI-D-14-00754.1, 2015

5   Castebrunet, H., Eckert, N., Giraud, G., Durand, Y., and Morin, S.: Projected changes of snow conditions and avalanche activity in a warming climate: the French Alps over the 2020–2050 and 2070–2100 periods, The Cryosphere, 8, 1673–1697, https://doi.org/10.5194/tc-8-1673-2014, 2014.

Dyrrdal, A.V., Isaksen, K., Hygen, H.O., and Meyer, N.K.: Changes in meteorological variables that can trigger natural hazards in Norway. Climate Research, 55: 153–165, 2012

Eckerstorfer, M., Malnes, E., and Müller, K.: A complete snow avalanche activity record from a Norwegian forecasting region using Sentinel-1 satellite-radar data. Cold Regions Science and Technology, 144, 39–51, ISSN 0165-232X, https://doi.org/10.1016/j.coldregions.2017.08.004, 2017

15   Engeset, R.V., Tveito, O.E., Alfnes, E., Mengistu, Z., Udnæs, H.C., Isaksen, K., and Førland, E.J.: Snow map system for Norway. In:Proc XXIII Nord Hydrol Conf, 8−12 Aug, Tallinn, NHP Report 48 (1), 112–121, 2004

Frauenfelder, R., Solheim, A., Isaksen, K., Romstad, B., Dyrrdal, A.V., Ekseth, K.H.H., Gangstø, R., Harbitz, A., Harbitz, C.B., Haugen, J.E., Hygen, H.O., Haakenstad, H., Jaedicke, C., Jónsson, Á., Klæboe, R., Ludvigsen, J., Meyer, N.M.,
20   Rauken, T., Sverdrup-Thygeson, K. & Aaheim, A.: Impacts of Extreme Weather Events on Infrastructure in Norway. Report 20091808-01-R. Oslo: Norwegian Geotechnical Institute, 2013

Geiger, R., Aron, R. H., and Todhunter, P.: The Climate Near the Ground, Springer Science and Business Media, 2012.

25   Gillett, N. P., Graf, H. F. and Osborn, T. J.: Climate Change and the North Atlantic Oscillation. In The North Atlantic Oscillation: Climatic Significance and Environmental Impact (eds J. W. Hurrell, Y. Kushnir, G. Ottersen and M. Visbeck). doi:10.1029/134GM09, 2013

Gustafson, K.: Icing Conditions on Different Pavement Structures. Swedish national road and traffic institute, VTI Särtryck
30   84. Retrieved from http://urn.kb.se/resolve?urn=urn:nbn:se:vti:diva-2263. 8 p, 1983.

Hanssen-Bauer, I., Førland, E.J., Hisdal, H., Mayer, S., Sandø, A.B., Sorteberg, A.: Climate in Svalbard 2100 – a knowledge base for climate adaptation. Norwegian Centre for Climate Services, Report 1/2019. 207 p, 2019

Hanssen-Bauer, I., Førland, E.J., Haddeland, I., Hisdal, H., Lawrence, D., Mayer, S., Nesje, A., Nilsen, J.E.Ø., Sandven, S., Sandø, A.B., Sorteberg, A. and Ådlandsvik, B.: Climate in Norway 2100 – a knowledge base for climate adaptation. Norwegian Centre for Climate Services, Report 1/2017, 2017.

5 Hendrikx, J., Owens, I., Carran, W., and Carran, A.: Avalanche activity in an extreme maritime climate: The application of classification trees for forecasting. Cold Regions Science and Technology 43 (1–2), 104–116, 2005. https://doi.org/10.1016/j.coldregions.2005.05.006.

Hestnes, E. and Jaedicke, C.: Global warming reduces the consequences of snow-related hazards. Proceedings, International
10 Snow Science Workshop, Innsbruck, Austria, 2018

Hisdal, H., Vikhamar Schuler, D., Førland, E.J., and Nilsen, I.B.: Klimaprofiler for fylker (Climate fact sheets for counties). NCCS report no. 3/2017, https://cms.met.no/site/2/klimaservicesenteret/rapporter-og-publikasjoner/_attachment/12110?_ts=15ddfbccf32, 2017

Holand, I.S. & Rød, J.K.: Kartlegging av infrastruktursårbarhet. In Bye, L.M, Lein, H. & Rød, J.K. (eds.) Mot en Farligere Fremtid? Om Klimaendringer, Sårbarhet og Tilpasning i Norge, 157–174. Trondheim: Akademika, 2013

Hovelsrud, G.K., Karlsson, M., and Olsen, J.: Prepared and flexible: Local adaptation strategies for avalanche risk. Cogent
20 Social Sciences 4:1460899, https://doi.org/10.1080/23311886.2018.1460899, 2018

IPCC – Field, C.B., V. Barros, T.F. Stocker, D. Qin, D.J. Dokken, K.L. Ebi, M.D. Mastrandrea, K.J. Mach, G.-K. Plattner, S.K. Allen, M. Tignor, and P.M. Midgley (Eds.) Available from Cambridge University Press, The Edinburgh Building, Shaftesbury Road, Cambridge CB2 8RU ENGLAND, 582 pp., 2012

Jacob, D., Petersen, J., Eggert, B., Alias, A., Christensen, O.B., Bouwer, L.M., Braun, A., Colette, A., Déqué, M., Georgievski, G., Georgopoulou, E., Gobiet, A., Menut, L., Nikulin, G., Haensler, A., Hempelmann, N., Jones, C., Keuler, K., Kovats, S., Kröner, N., Kotlarski, S., Kriegsmann, A., Martin, E., van Meijgaard, E., Moseley, C., Pfeifer, S., Preuschmann, S., Radermacher, C., Radtke, K., Rechid, D., Rounsevell, M., Samuelsson, P., Somot, S., Soussana, J.-F., Teichmann, C.,
30 Valentini, R., Vautard, R., Weber, B., Yiou, P.: EURO-CORDEX: New high-resolution climate change projections for European impact research. Regional Environmental Change, 14 (2), pp. 563–578, 2014

Jacobsen, J. K. S., Leiren, M. D., and Saarinen, J.: "Natural hazard experiences and adaptations." Norwegian Journal of Geography 70 (5): 292–305. doi:10.1080/00291951.2016.1238847, 2016

Jaedicke, C., Solheim, A., Blikra, L.H., Stalsberg, K., Sorteberg, A., Aaheim, A., Kronholm, K., Vikhamar-Schuler, D., Isaksen, K., Sletten, K., Kristensen, K., Barstad, I., Melchiorre, C., Høydal, Ø.A. and Mest, H.: Spatial and temporal variations of Norwegian geohazards in a changing climate, the GeoExtreme project. Nat Hazards Earth Syst Sci 8: 893−904, 2008

Jaedicke, C., Lied, K., and Kronholm, K.: Integrated database for rapid mass movements in Norway, Nat. Hazards Earth Syst. Sci., 9, 469–479, https://doi.org/10.5194/nhess-9-469-2009, 2009

Jamieson, B., Bellaire, S., and Sinickas, A.: Climate change and planning for snow avalanches in transportation corridors in
10 western Canada, in: GEO Ottawa 2017, https://schulich.ucalgary.ca/asarc/files/asarc/snowavalanchetrendstransporationcorridors_geoottawa2017_ jamiesonetal_1july2017.pdf, 2017.

Kalsnes, B., Nadim, F., Hermanns, R., Hygen, H., Petkovic, G., Dolva, B., and Høgvold, D.: Landslide risk management in
15 Norway K.H.S. Lacasse, L. Picarelli (Eds.), Slope safety preparedness for impact of climate change, CRC Press, Boca Raton, FL, pp. 215–252, 2016

Kerguillec, R.: Seasonal distribution and variability of atmospheric freeze/thaw cycles in Norway over the last six decades (1950–2013). Boreas, Vol. 44, pp. 526–542.10.1111/bor.12113. ISSN 0300-9483, 2015

Kristiensen, L.L., Jensen, O.A., Devoli, G., Rustad, B.K., Verhage, A., Viklund, M., and Larsen, J.O.: Terminologi for naturfare. (In English: Terminology for natural hazards), NVE report 90/2015, 2015

Kronholm, K., Vikhamar-Schuler, D., Jaedicke, C., Isaksen, K., Sorteberg, A., and Kristensen, K: Forecasting snow
25 avalanche days from meteorological data using classification trees; Grasdalen, western Norway., 2006

Lee, S.-S., Lee, J.-Y., Wang, B., Ha, K.-J., Heo, K.-Y., Jin, F.-F., Straus, D., and Shukla, J.: Interdecadal changes in the storm track activity over the North Pacific and North Atlantic. Climate Dynamics. 39. 313–327. 10.1007/s00382-011-1188-9, 2012

Leiren, M. D. & Jacobsen, J. K. S.: Silos as barriers to public sector climate adaptation and preparedness: Insights from road closures in Norway. Local Government Studies, 44:4, 492–511. doi:10.1080/03003930.2018.1465933, 2018

Lussana, C., Saloranta, T., Skaugen, T., Magnusson, J., Tveito, O.-E., and Andersen, J.: seNorge2 daily precipitation, an observational gridded dataset over Norway from 1957 to the present day. Earth Syst. Sci. Data, 10, 235–249, https://doi.org/10.5194/essd-10-235-2018, 2018

5 Norwegian Ministry of Climate and Environment. Klimatilpasning i Norge (White paper 33 (2012–2013) on climate adaptation in Norway). Norwegian Ministry of Climate and Environment, Oslo, Norway, 2013. https://www.regjeringen.no/contentassets/e5e7872303544ae38bdbdc82aa0446d8/no/pdfs/stm201220130033000dddpdfs.pdf

Naaim M., Durand, Y., Eckert N., and Chambon G.: Dense avalanche friction coefficients: Influence of physical properties
10 of snow. J Glaciol 59: 771–782, 2013

Naaim, M., Eckert, N., Giraud, G., Faug, T., Chambon, G., Naaim-Bouvet, F., and Richard D.: Impact of climate warming on avalanche activity in French Alps and increase of proportion of wet snow avalanches. La Houille Blanche (6) 12–20. DOI: 10.1051/lhb/2016055, 2016

Norwegian Geotechnical Institute NGI (2013): Impacts of extreme weather events on infrastructure in Norway (InfraRisk) - Final report to NFR-prosjekt 200689. Frauenfelder, R., Solheim, A., Isaksen, K., Romstad, B., Dyrrdal, A.V., Gangstø, R., Harbitz, A., Harbitz, C.B., Haugen, J.E., Hygen, H.O., Haakenstad, H., Jaedicke, C., Jónsson, Á., Klæboe, R., Ludvigsen, J., Meyer, N.M., Rauken, R., Sverdrup-Thygeson, K., Aaheim, A. NGI rapport nr. 20091808-
20 01-R. 94 s. + Appendix

NVE: Sikkerhet mot skred i bratt terreng (in English: "Avalanche safety in steep terrain"). Veileder nr. 8 2014. Norwegian water resources and Energy Directorate (NVE), 2014. http://publikasjoner.nve.no/veileder/2014/veileder2014_08.pdf

25 Pall, P., Tallaksen, L.M., and Stordal, F.: A climatology of rain-on-snow events for Norway. Journal of Climate, 32(20), 6995–7016, 2019. https://doi.org/10.1175/JCLI-D-18-0529.1

Parding, K. and Benestad, R.: Storm activity and climate change in northern Europe. MET report 10/16, 2016

30 Polyakov, I.V., Bekryaev, R.V., Alekseev, G.V., Bhatt, U.S., Colony, R.L., Johnson, M.A., Maskshtas, A.P., and Walsh, D.: Variability and Trends of Air Temperature and Pressure in the Maritime Arctic, 1875–2000. J. Climate, 16, 2067–2077, https://doi.org/10.1175/1520-0442(2003)016<2067:VATOAT>2.0.CO;2, 2003

Reistad, M., Breivik, Ø., Haakenstad, H., Aarnes, O.J., Furevik, B.R., and Bidlot, J.-R.: A high-resolution hindcast of wind and waves for the North Sea, the Norwegian Sea, and the Barents Sea, J. Geophys. Res., 116, C05019, doi:10.1029/2010JC006402, 2011

5   Sorteberg, A., Kvamstø, N.G., and Byrkjedal, Ø.: Wintertime Nordic Seas Cyclone Variability and its Impact on Oceanic Volume Transports into the Nordic Seas. In The Nordic Seas: An Integrated Perspective (eds H. Drange, T. Dokken, T. Furevik, R. Gerdes and W. Berger). doi:10.1029/158GM10, 2013

Saloranta, T.: New version (v.1.1.1) of the seNorge snow model and snow maps for Norway. NVE report 6-2014, 2014

Sandersen, F., Bakkehøi, S., Hestnes, E., Lied, K.: The influence of meteorological factors on the initiation of debris flows, rockfalls, rockslides and rock mass stability. In: Senneset K (ed) Proc 7th Symp Landslides, Trondheim, p 97−114, 1996

Schweizer, J., Jamieson, J. B., and Schneebeli, M.: Snow avalanche formation, Rev. Geophys., 41, 1016,
15   doi:10.1029/2002RG000123, 4, 2003

Sinickas, A., Jamieson, B., and Maes, M. A.: Snow avalanches in western Canada: investigating change in occurrence rates and implications for risk assessment and mitigation, Structure and Infrastructure Engineering: 12, 490–498, doi:10.1080/15732479.2015.1020495, 2016.

Sjømatklyngen Senja: Godstransport i sjømatregion Senja (In English: Freight transportation in Senja seafood region). Finnsnes: Sjømatklyngen Senja, 2017

Sovilla, B., Kern, M., and Schaer, M.: Slow drag in wet-snow avalanche flow. J Glaciol 56, 587–592, 2010

Statens vegvesen: Håndbok V138 Veger og snøskred (Roads and snow avalanches), 2014

Tveito O.E., Udnæs, H.C., Mengistu, Z., Engeset, R., and Førland, E.J.: New snow maps for Norway. In: Proc XXII Nord Hydrol Conf, 4−7 Aug 2002, Røros, NHP Report 47, 527–532, 2002

Thornes, J.E.: Thermal mapping and road-weather information systems for highway engineers. Highway Meteorology. E and FN Spon: London, England, 39–67, 1991

Vikhamar-Schuler, D., Isaksen, K., Haugen, J.E., Tømmervik, H., Luks, B., Schuler, T., and Bjerke J.: Changes in winter warming events in the Nordic Arctic Region. Journal of Climate 29, doi: 10.1175/JCLI-D-15-0763.1, 2016

Wong, W.K., Haddeland, I., Lawrence, D., and Beldring, S.: Gridded 1 x 1 km climate and hydrological projections for
5   Norway. NVE report No. 59 – 2016, 2016

Yue, S. and Pilon, P.: A comparison of the power of the t test, Mann-Kendall and bootstrap tests for trend detection. Hydrol Sci J 49, 21−37, 2004

10   Zappa, G., Shaffrey, L.C., and Hodges, K.I.: The ability of CMIP5 models to simulate North Atlantic extratropical cyclones. Journal of Climate 26, 5379–5396, 2013
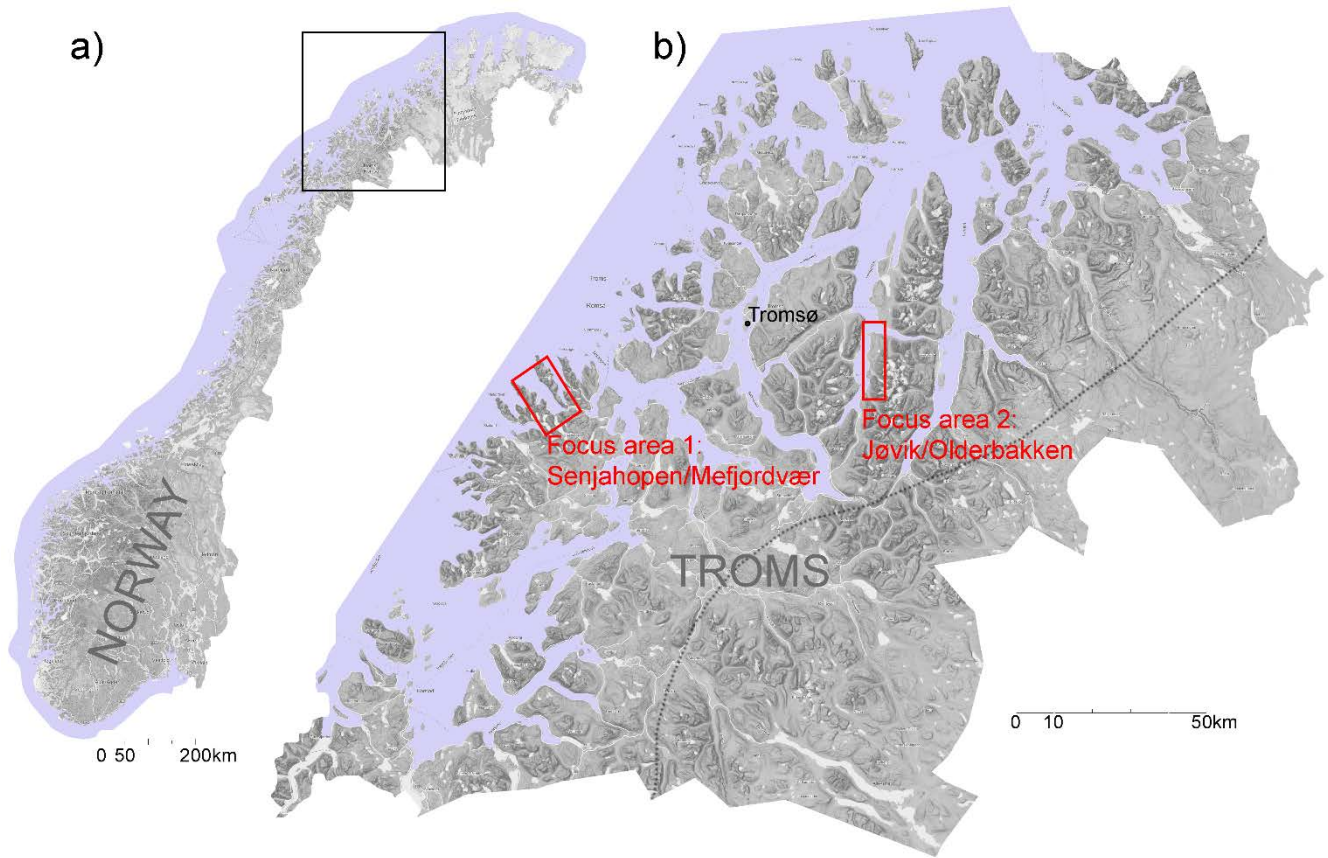
Figure 1: Map of Norway (left) and Troms (right), with inland and coastal regions separated by the stippled line, and our two focus areas, Focus area 1 and Focus area 2 in red squares.

Winter temperature and precipitation
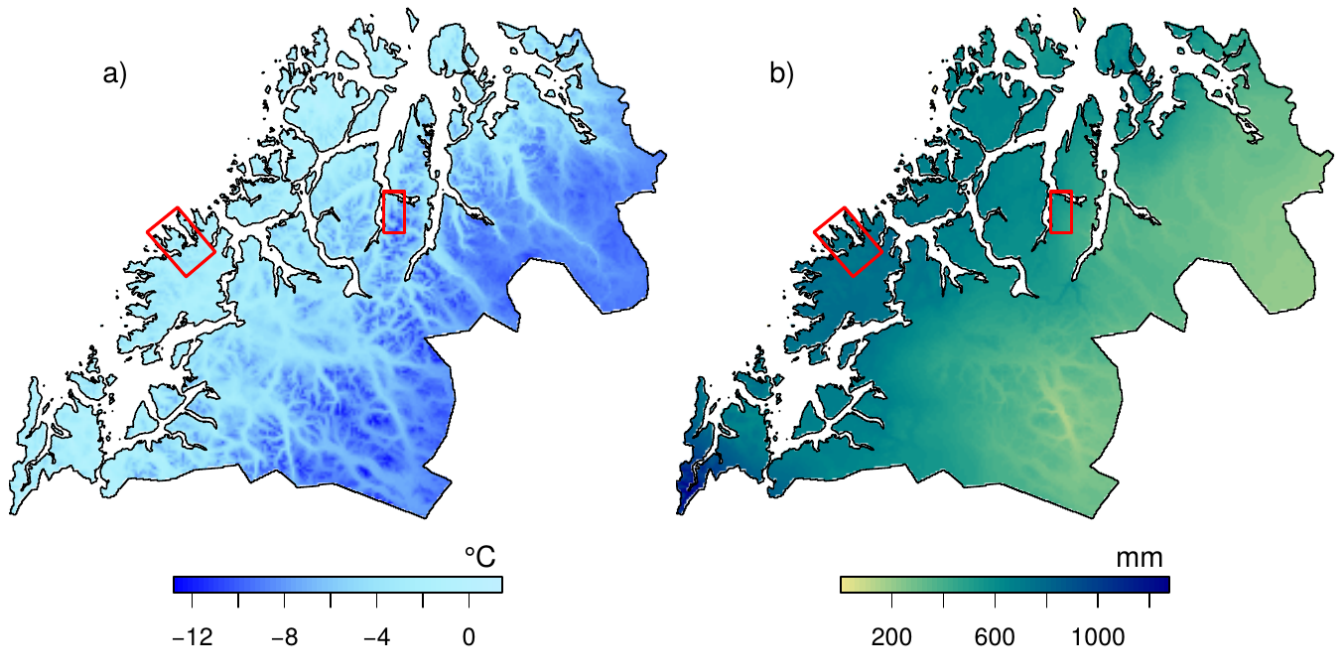
Figure 2: Mean winter temperature and total winter precipitation averaged over the period 1981–2010.
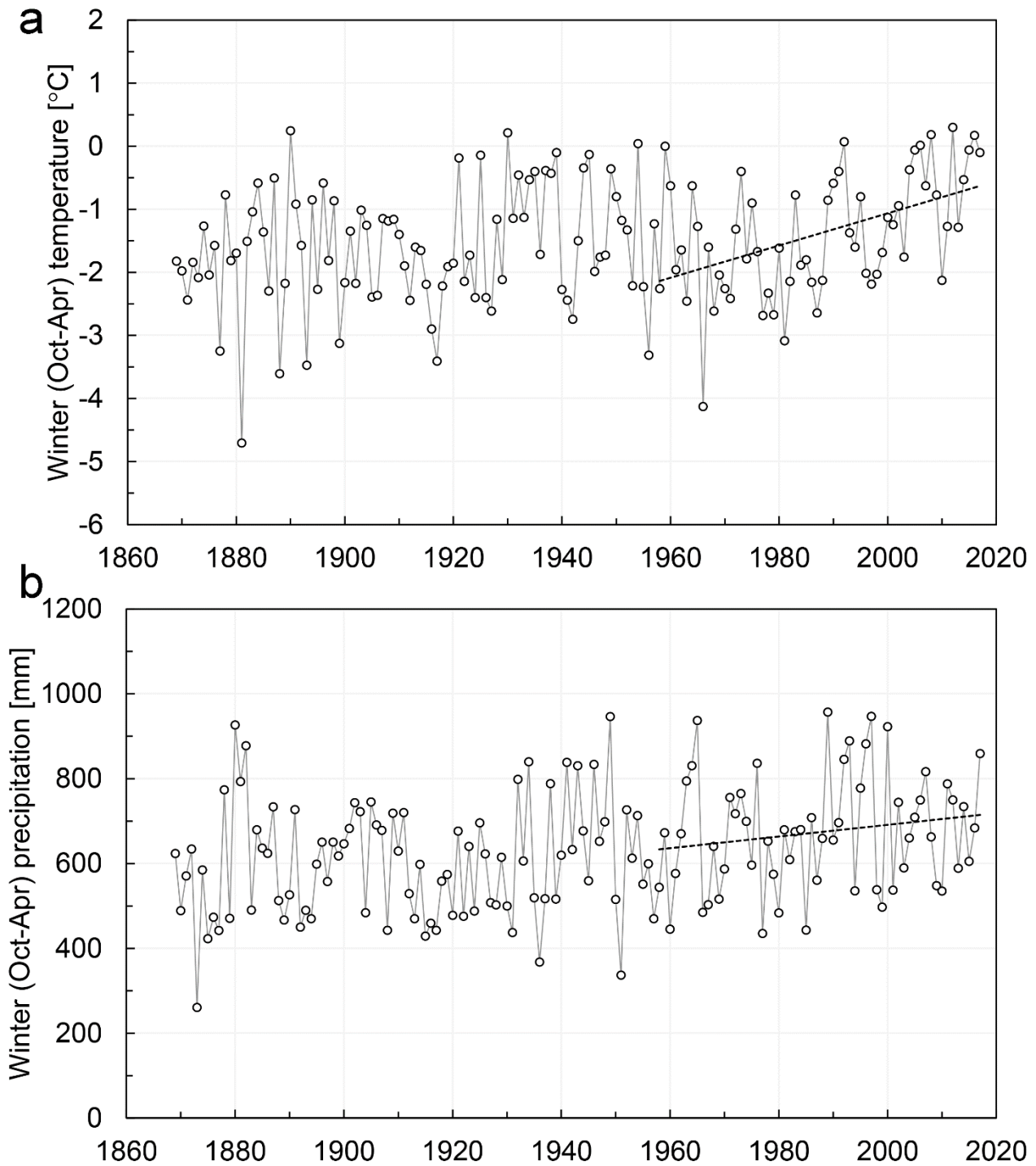
Figure 3: Mean winter temperature (a) and total winter precipitation (b) measured at Tromsø meteorological station in the period 1867-2017. The stippled line indicates the trend in the period 1958-2017.
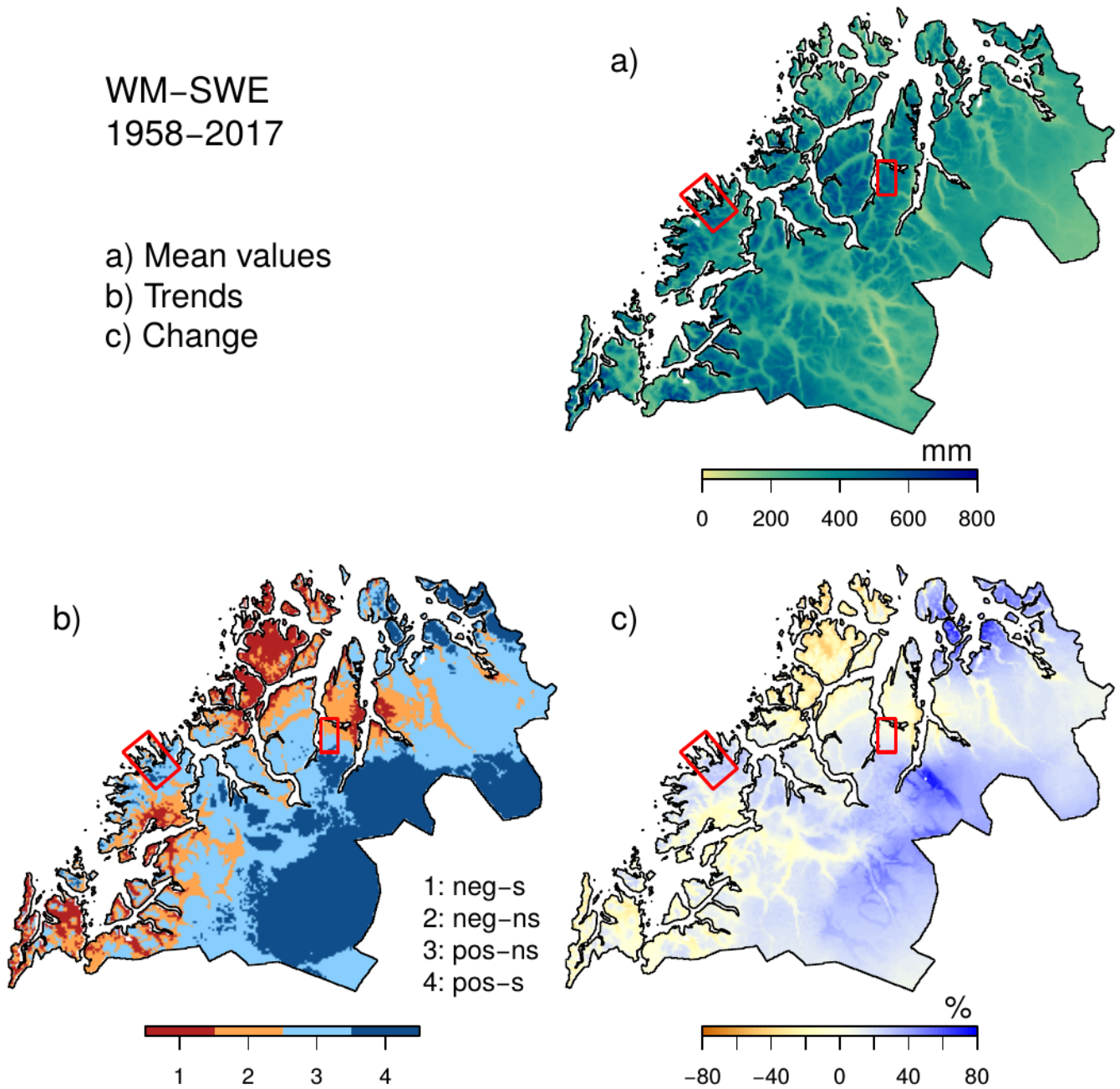
Figure 4: Mean values (a), trends (b) and changes (c) in winter (Oct–Apr) maximum snow water equivalent (SWE) for the period 1958–2017. In b), positive trends are illustrated in blue and negative trends in red; dark red and blue colors represent statistically negative and positive significant (s) trends, respectively. Light colors represent statistically not-significant (ns) trends. In c), percentage changes between the two 30-year periods 1958–1987 and 1988–2017 are shown.
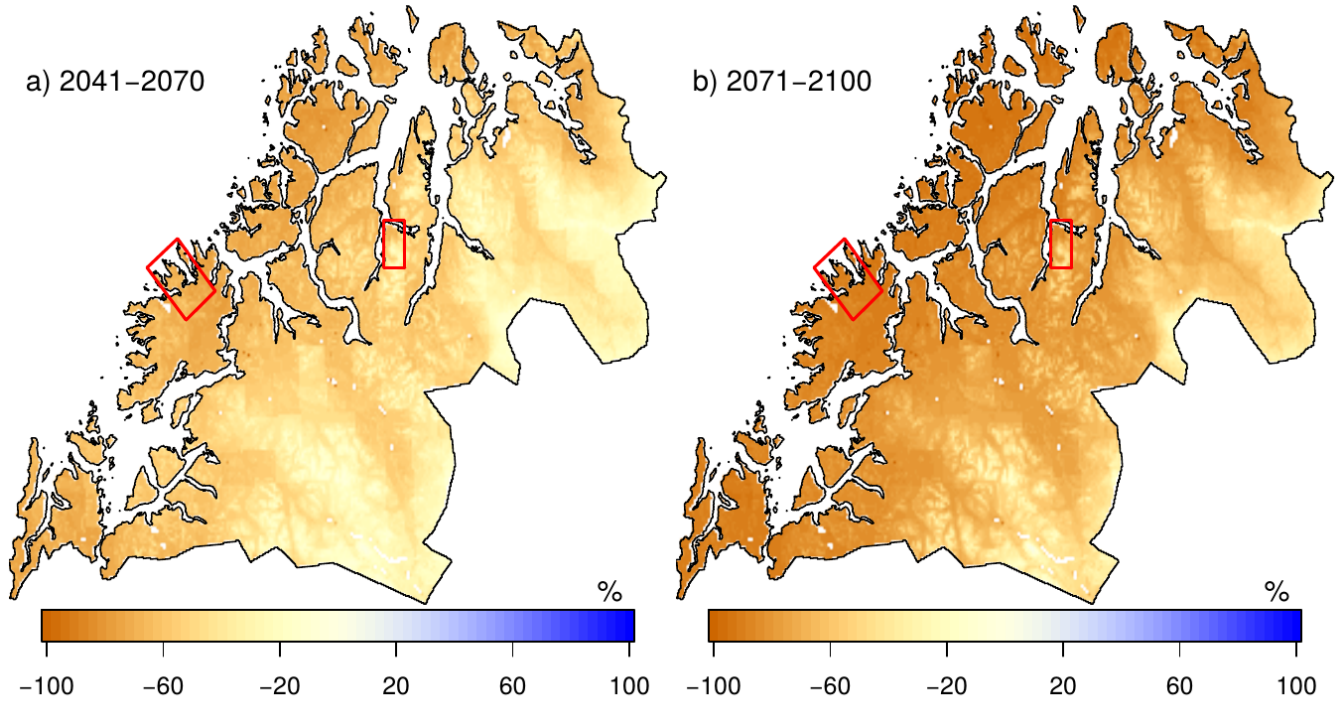
Figure 5: Projected change in maximum snow water equivalent (SWE) during winter (Oct–Apr) between 1981-2010 and a) near future (2041-2070); b) far future (2071-2100.
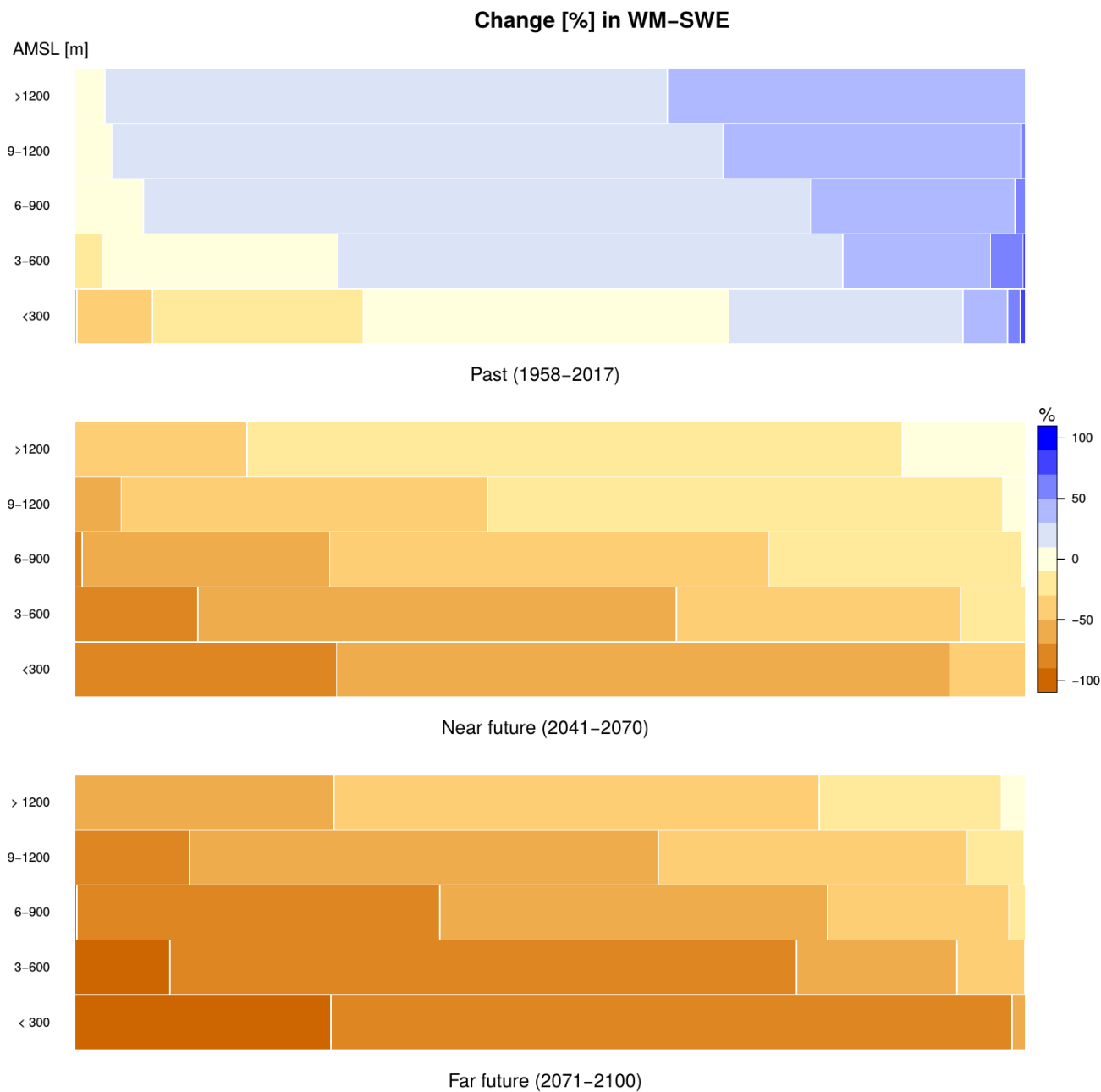
Figure 6: Percentage change in winter maximum SWE in different elevation levels for: historical period (change between 1958-1987 and 1988-2017; upper panel), near future (change between 1981-2010 and 2041-2070; middle panel) and far future (change between 1981-2010 and 2071-2100; lower panel). The length of the colored bars represent the fraction of grid cells within the different intervals given by the legend.
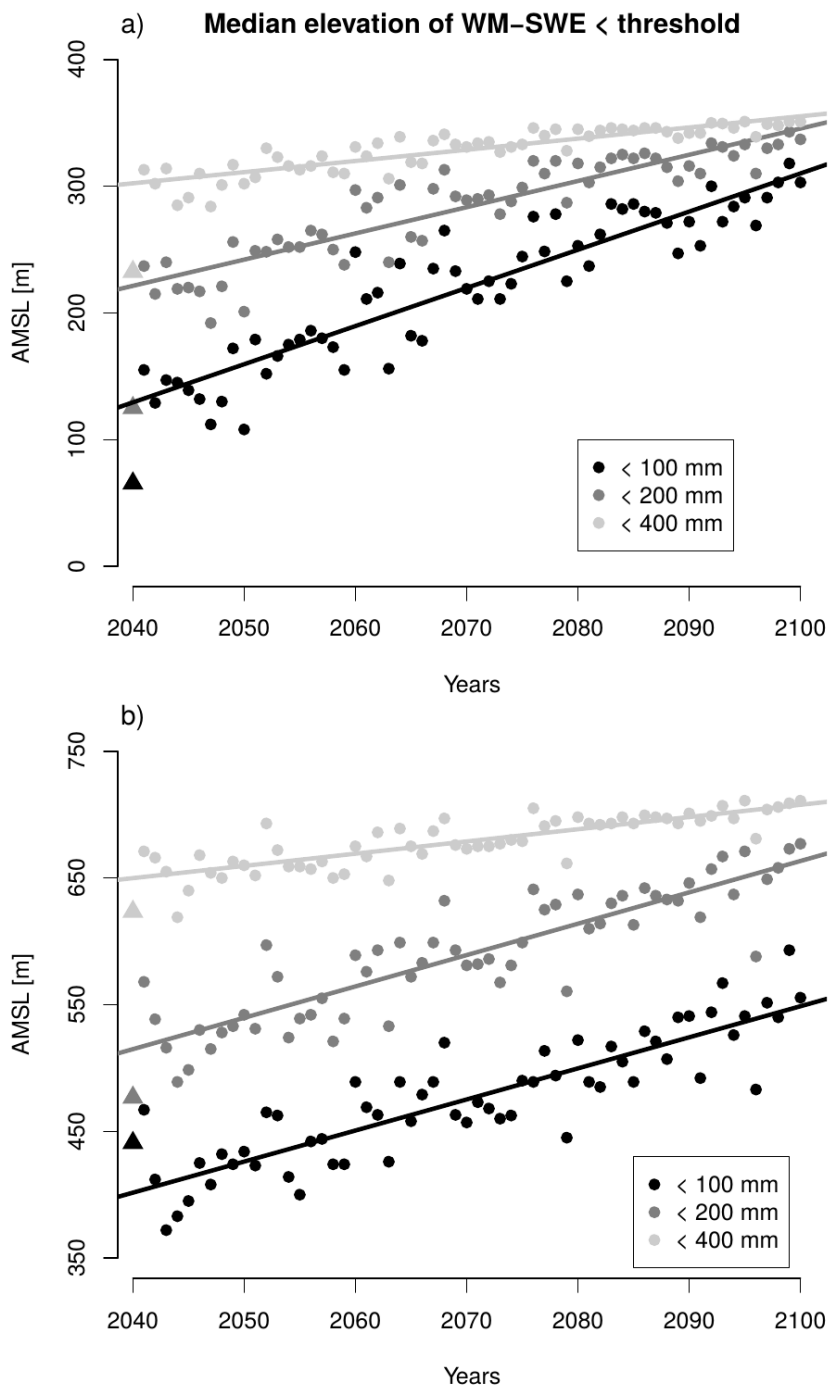
Figure 7: Projected future development in median elevation where winter maximum SWE is below 100 mm (black), 200 mm (dark grey) or 400 mm (light grey). a) Coast and b) inland (see map in Fig.1). Mean values for the period 1981-2010 are indicated as triangles.
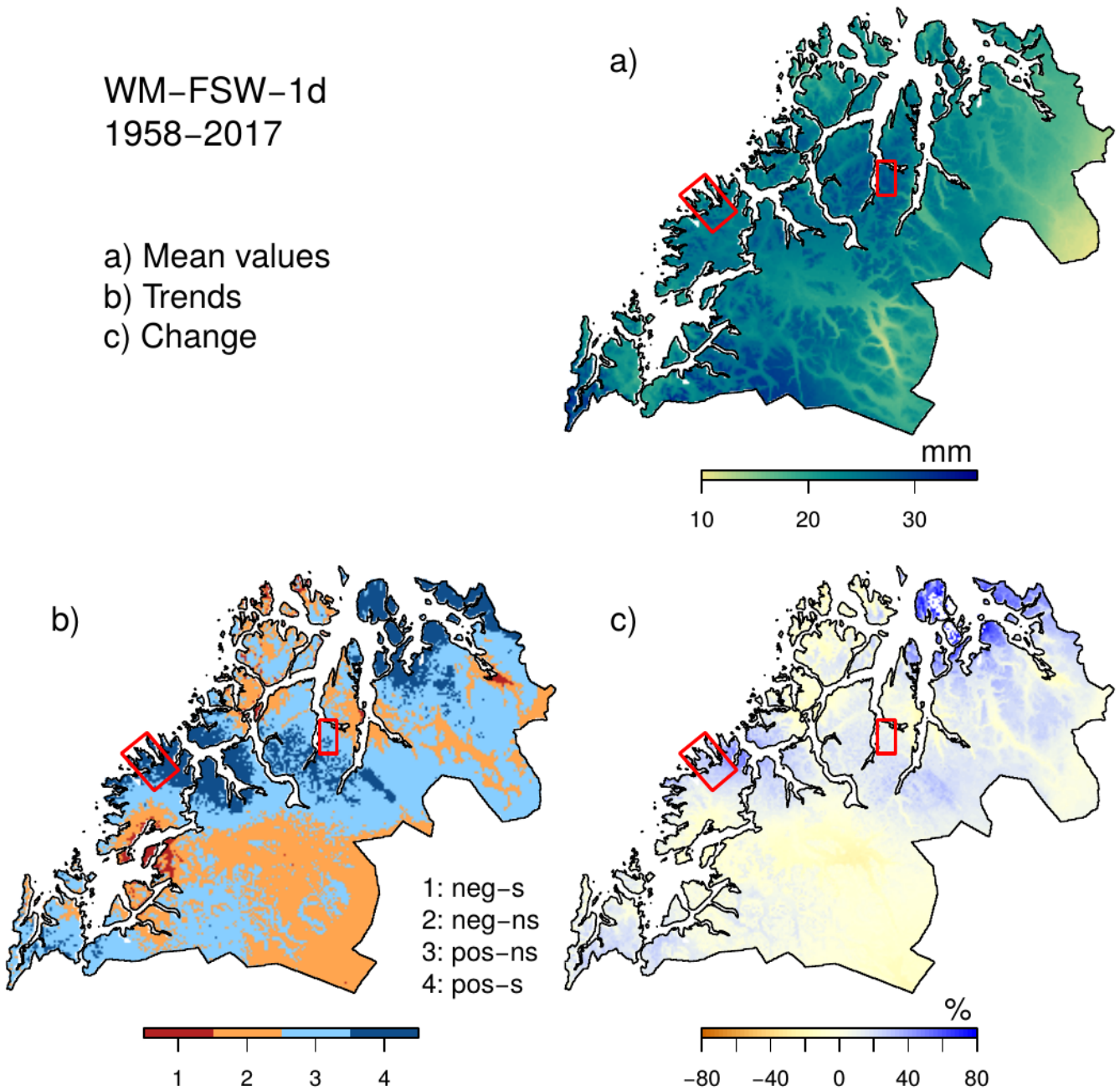
Figure 8: Maximum 1-day snowfall during winter (Oct–Apr) for the period 1958-2017, based on maximum fresh snow water equivalent for 1-day duration (WM-FSW-1d). Mean values (a), trends (b) and changes are shown in the same way as in Fig.4.
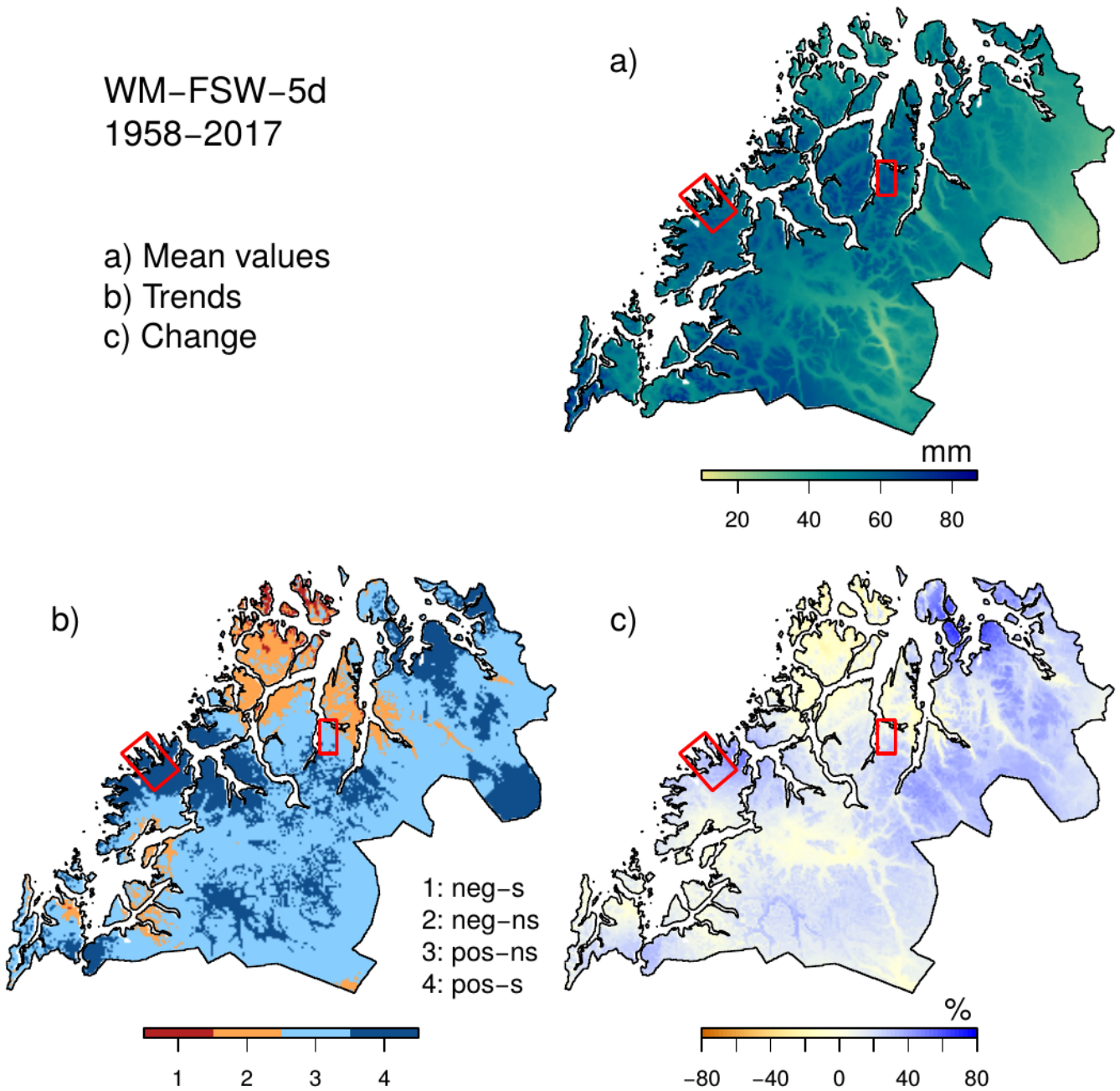
Figure 9: Maximum 5-day snowfall during winter (Oct–Apr), based on maximum fresh snow water equivalent for 5-day duration (WM-FSW-5d). Absolute mean values (a), trends (b) and changes are shown in the same way as in Fig.4.

Figure 10: Projected change in maximum 1-day snowfall during winter (Oct–Apr) between 1981-2010 and a) near future (2041-2070); b) far future (2071-2100, based on maximum fresh snow water equivalent for 1-day duration (WM-FSW-1d).

Projected change in WM–FSW–5d, compared to 1981–2010
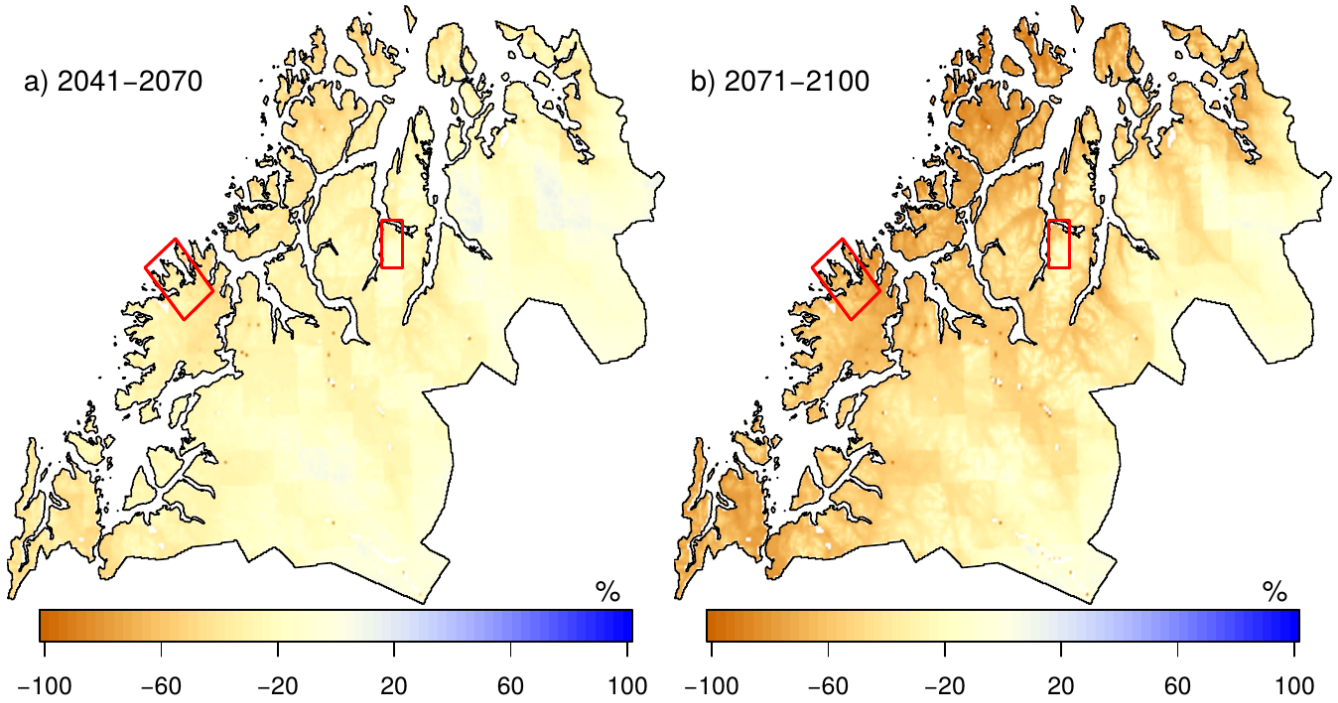
Figure 11: Projected change in maximum 5-day snowfall during winter (Oct–Apr) between 1981-2010 and a) near future (2041-2070); b) far future (2071-2100, based on maximum fresh snow water equivalent for 5-day duration (WM-FSW-5d).
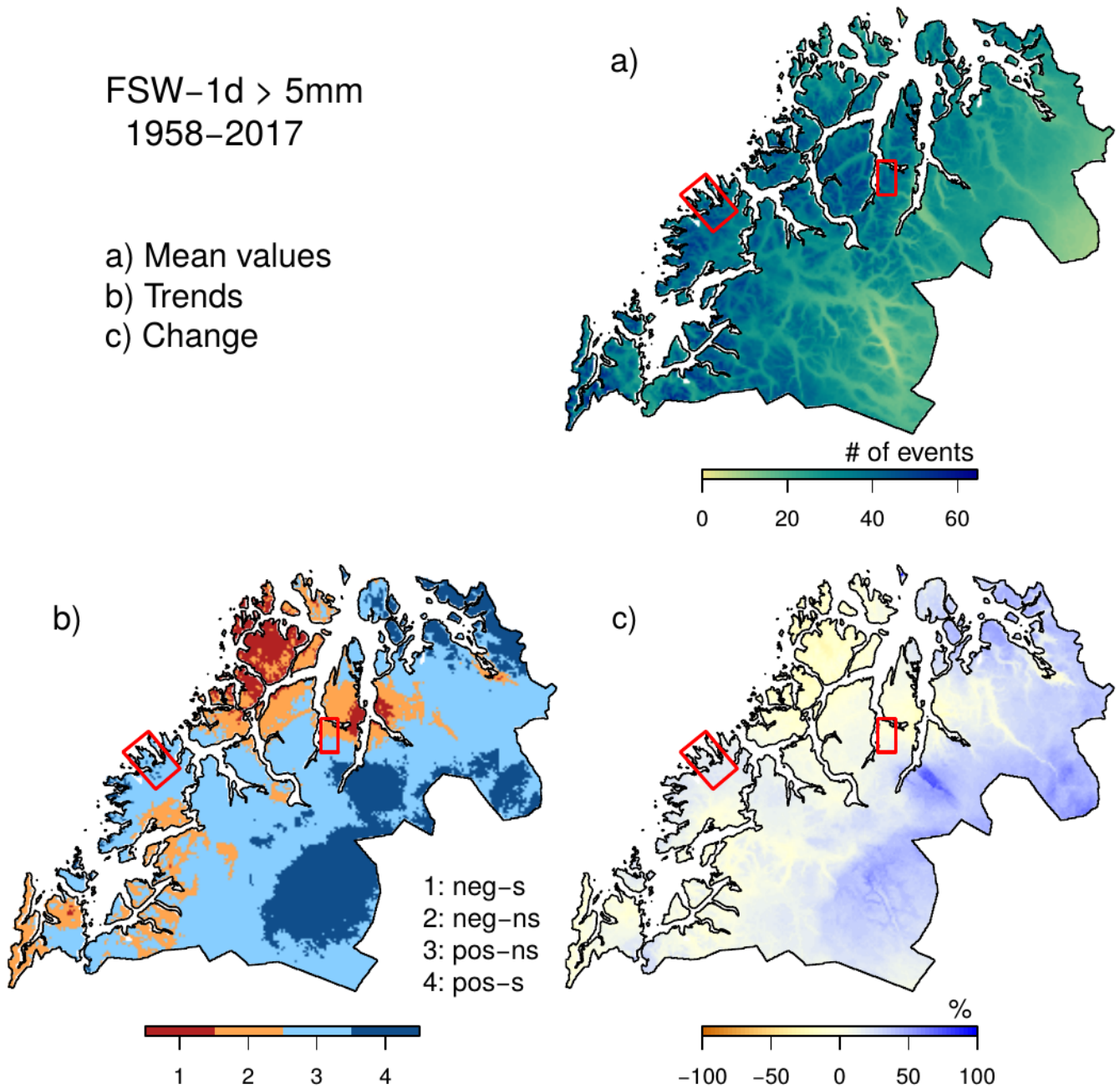
Figure 12: Frequency of 1-day snowfall exceeding 5 mm during winter (Oct-Apr) for the period 1958-2017, based on fresh snow water equivalent for 1-day duration (FSW-1d > 5 mm). Mean values (a), trends (b) and changes are shown in the same way as in Fig.4.

Projected change in FSW−1d > 5mm, compared to 1981−2010
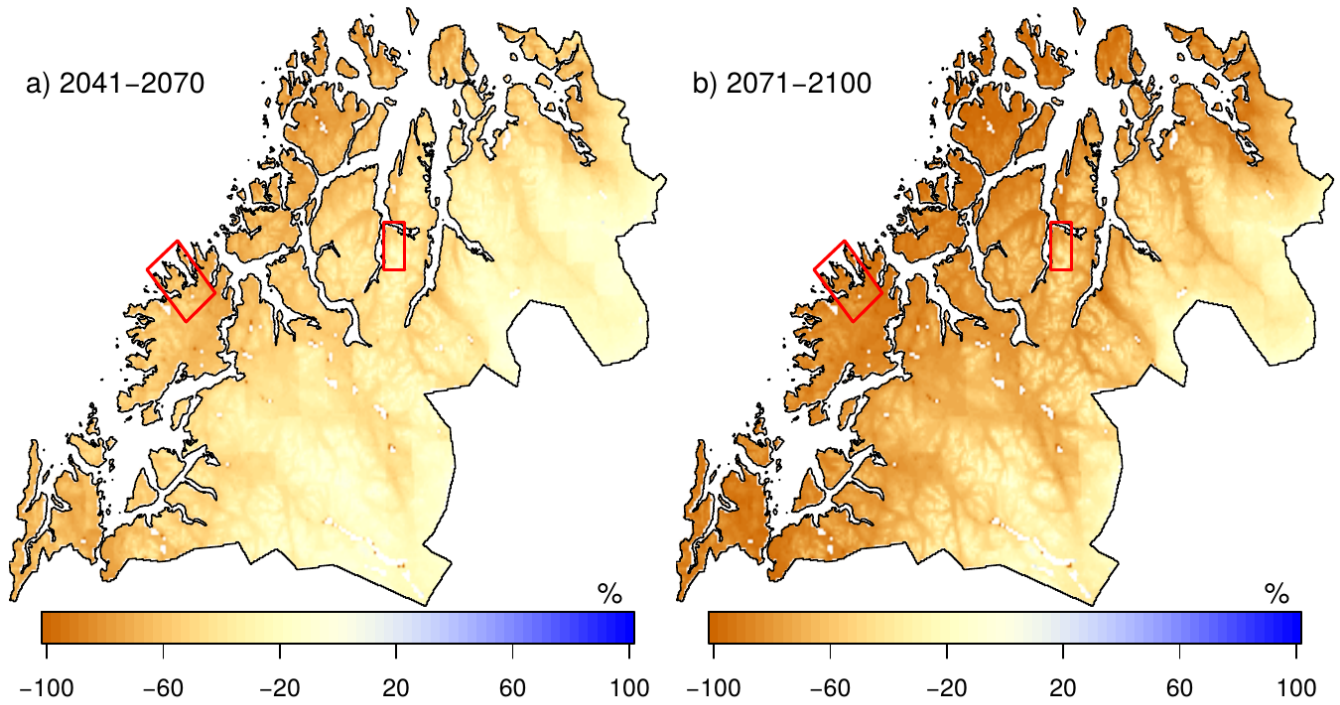
Figure 13: Projected change in the frequency of 1-day snowfall exceeding 5 mm during winter (Oct-Apr) between 1981-2010 and a) near future (2041-2070) and b) far future (2071-2100), based on fresh snow water equivalent for 1-day duration (FSW-1d > 5 mm).
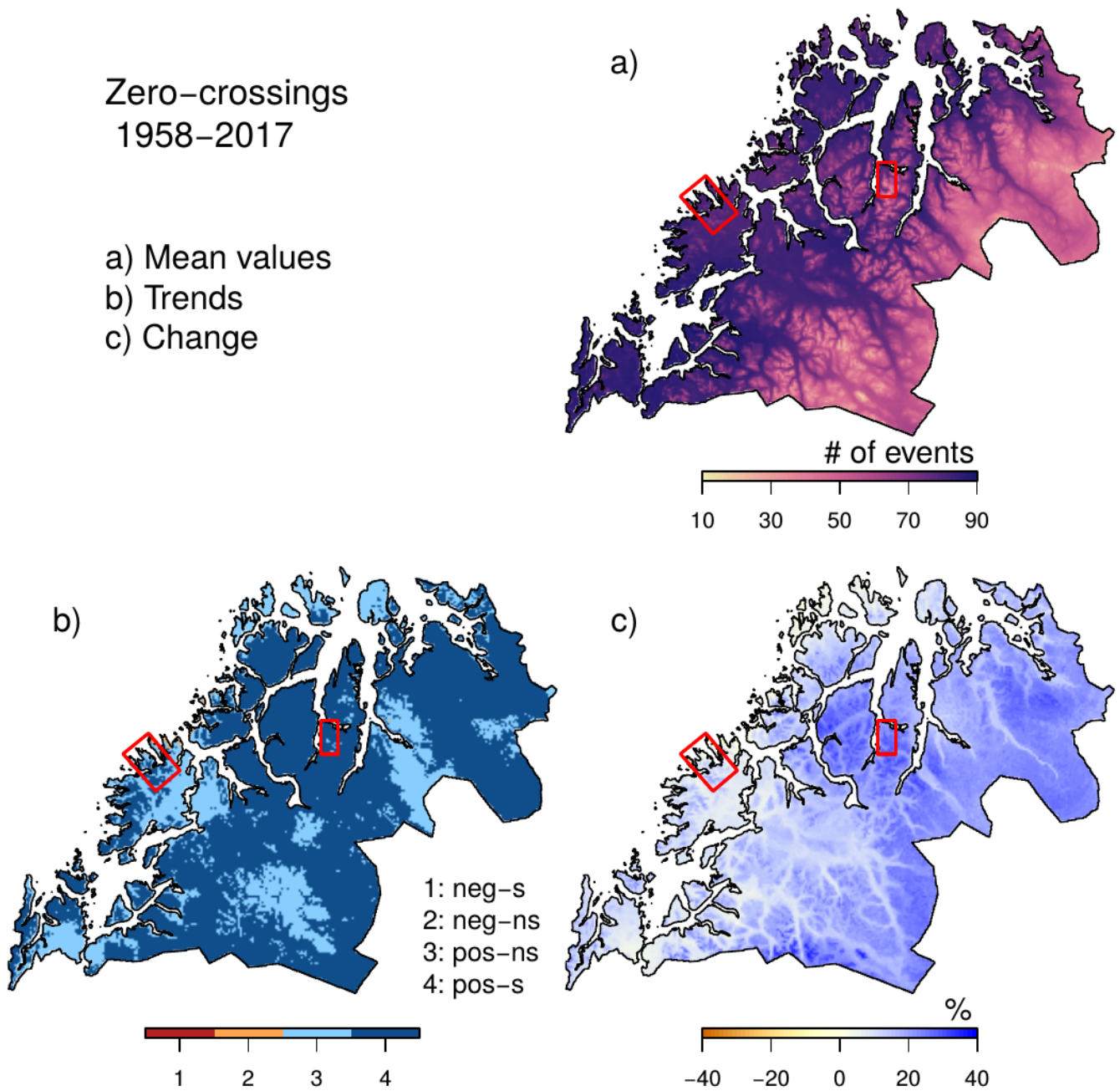
Figure 14: Frequency of zero-crossings during winter (Oct-Apr) for the period 1958-2017, based on minimum and maximum daily temperature. Mean values (a), trends (b) and changes are shown in the same way as in Fig.4.

Figure 15: Projected change in the frequency of zero-crossings during winter (Oct-Apr) between 1981-2010 and a) near future (2041-2070) and b) far future (2071-2100), based on minimum and maximum temperature.
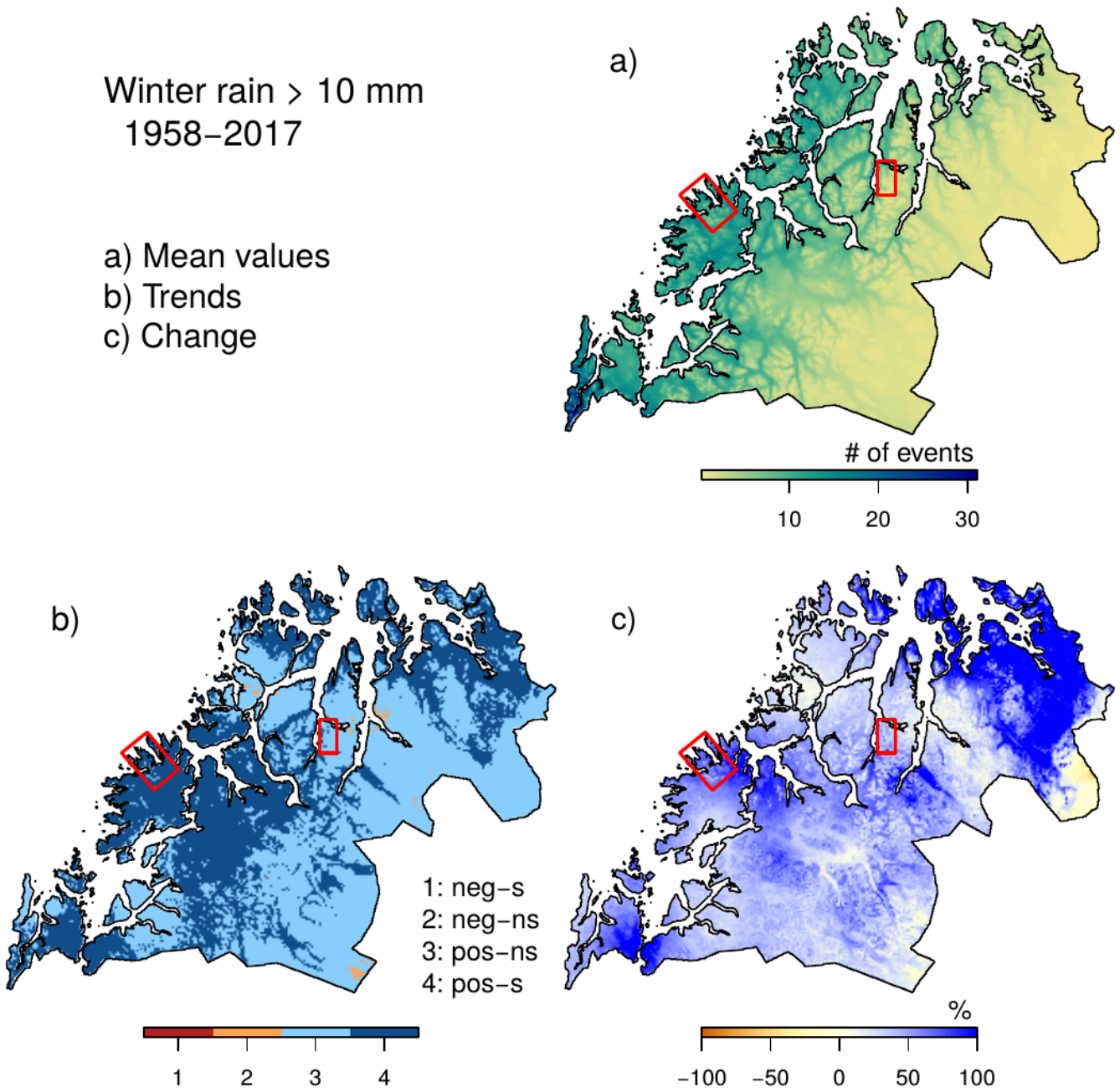
Figure 16: Frequency of rainfall events exceeding 10 mm during winter (Oct-Apr) for the period 1958-2017, based on minimum and maximum daily temperature. Mean values (a), trends (b) and changes are shown in the same way as in Fig.4.

Figure 17: Projected change in the frequency of rainfall events exceeding 10 mm during winter (Oct-Apr) between 1981-2010 and a) near future (2041-2070) and b) far future (2071-2100). Note that the legend differs from other figures, going from 0 to 400%.

Appendix

Table A1: GCM/RCM combinations in the EURO-CORDEX ensemble, where the first column indicates the name of the GCM and the first row indicates the name of the RCM.

GCM/RCM	CNRM	EC-EARTH	HADGEM	IPSL	MPI
CCLM	x	x			x
RCA	x	x	x	x	x
HIRHAM		x			
RACMO		x			